JPn Neuroscience
The Journal of Physiology
J Physiol 591.10 (2013) pp 2443–2462

Mitochondria and plasma membrane Ca^{2+}-ATPase control presynaptic Ca^{2+} clearance in capsaicin-sensitive rat sensory neurons

Leonid P. Shutov[1], Man-Su Kim[1,2], Patrick R. Houlihan[1], Yuliya V. Medvedeva[1] and Yuriy M. Usachev[1]

[1]*Department of Pharmacology, University of Iowa Carver College of Medicine, Iowa City, IA 52242, USA*
[2]*College of Pharmacy, Inje University, Gimhae, Republic of Korea*

Key points

- The first sensory synapse formed between the central processes of primary afferents and dorsal horn neurons plays an important role in controlling the flow of nociceptive information from the periphery to the CNS, and plasticity at this synapse contributes to centrally mediated pain hypersensitivity.
- Although exocytosis and synaptic plasticity are regulated by presynaptic Ca^{2+}, the mechanisms underlying presynaptic Ca^{2+} signalling at the first sensory synapse are not well understood.
- In this study we show that the plasma membrane Ca^{2+}-ATPase and mitochondria are the major regulators of presynaptic Ca^{2+} signalling in capsaicin-sensitive dorsal root ganglion neurons accounting for ∼47 and ∼40% of presynaptic Ca^{2+} clearance, respectively.
- Quantitative analysis of changes in cytosolic and mitochondrial Ca^{2+} concentrations demonstrates that the mitochondrial Ca^{2+} uniporter is highly sensitive to cytosolic Ca^{2+} at this synapse.
- These results help us understand presynaptic mechanisms at the first sensory synapse.

Abstract The central processes of primary nociceptors form synaptic connections with the second-order nociceptive neurons located in the dorsal horn of the spinal cord. These synapses gate the flow of nociceptive information from the periphery to the CNS, and plasticity at these synapses contributes to centrally mediated hyperalgesia and allodynia. Although exocytosis and synaptic plasticity are controlled by Ca^{2+} at the release sites, the mechanisms underlying presynaptic Ca^{2+} signalling at the nociceptive synapses are not well characterized. We examined the presynaptic mechanisms regulating Ca^{2+} clearance following electrical stimulation in capsaicin-sensitive nociceptors using a dorsal root ganglion (DRG)/spinal cord neuron co-culture system. Cytosolic Ca^{2+} concentration ($[Ca^{2+}]_i$) recovery following electrical stimulation was well approximated by a monoexponential function with a τ∼2 s. Inhibition of sarco-endoplasmic reticulum Ca^{2+}-ATPase did not affect presynaptic $[Ca^{2+}]_i$ recovery, and blocking plasmalemmal Na^+/Ca^{2+} exchange produced only a small reduction in the rate of $[Ca^{2+}]_i$ recovery (∼12%) that was independent of intracellular K^+. However, $[Ca^{2+}]_i$ recovery in presynaptic boutons strongly depended on the plasma membrane Ca^{2+}-ATPase (PMCA) and mitochondria that accounted for ∼47 and 40%, respectively, of presynaptic Ca^{2+} clearance. Measurements using a mitochondria-targeted Ca^{2+} indicator, mtPericam, demonstrated that presynaptic mitochondria accumulated Ca^{2+} in response to electrical stimulation. Quantitative analysis revealed that the mitochondrial Ca^{2+} uptake is highly sensitive to presynaptic $[Ca^{2+}]_i$ elevations, and occurs at $[Ca^{2+}]_i$ levels as low as ∼200–300 nM. Using RT-PCR, we detected expression of several putative mitochondrial Ca^{2+}

DOI: 10.1113/jphysiol.2012.249219

transporters in DRG, such as MCU, Letm1 and NCLX. Collectively, this work identifies PMCA and mitochondria as the major regulators of presynaptic Ca^{2+} signalling at the first sensory synapse, and underlines the high sensitivity of the mitochondrial Ca^{2+} uniporter in neurons to cytosolic Ca^{2+}.

(Received 27 November 2012; accepted after revision 30 January 2013; first published online 4 February 2013)
Corresponding author Y. M. Usachev: Department of Pharmacology, University of Iowa Carver College of Medicine, 2-340F BSB, 51 Newton Road, Iowa City, IA 52242, USA. Email: yuriy-usachev@uiowa.edu

Abbreviations AraC, cytosine β-D-arabinofuranoside; $[Ca^{2+}]_i$, cytosolic Ca^{2+} concentration; $[Ca^{2+}]_{mt}$, mitochondrial Ca^{2+} concentration; CaM, calmodulin; CPA, cyclopiazonic acid; DRG, dorsal root ganglia; $\Delta\Psi_{mt}$, mitochondrial membrane potential; EPSC, excitatory postsynaptic current; ER, endoplasmic reticulum; FCCP, carbonyl cyanide *p*-trifluoromethoxyphenylhydrazone; MCU, mitochondrial Ca^{2+} uniporter; MICU1, mitochondrial calcium uptake 1; Letm1, leucine zipper EF hand-containing transmembrane protein; LTP, long-term potentiation; NCX, Na^+/Ca^{2+} exchanger; NCKX, K^+-dependent Na^+/Ca^{2+} exchanger; NCLX, $Na^+/Ca^{2+}/Li^+$ exchanger; PKA, protein kinase A; PKC, protein kinase C; PMCA, plasma membrane Ca^{2+}-ATPase; Rhod10K, tetramethylrhodamine 10K dextran; RuR, ruthenium red; SC, spinal cord; SERCA, sarco-endoplasmic reticulum Ca^{2+}-ATPase; Tg, thapsigargin; TRPV1, transient receptor potential vanilloid 1.

Introduction

Primary nociceptive neurons send their central processes to the dorsal horn of the spinal cord where they form glutamatergic synaptic connections with the second-order nociceptive neurons (Woolf & Salter, 2006; Kuner, 2010). This synaptic connection, often referred to as the first sensory synapse, plays a critical role in controlling the flow of nociceptive information from the periphery into the CNS. Inhibiting transmission at this synapse with blockers of voltage-gated Ca^{2+} channels or opioids produces analgesic effects (Cao, 2006; McGivern, 2006; Heinke *et al.* 2011), whereas facilitation of sensory transmission through various forms of synaptic plasticity (including wind-up, central sensitization and long-term potentiation) contributes to the pain hypersensitivity associated with inflammation or nerve injury (Ji *et al.* 2003; Woolf & Salter, 2006; Kuner, 2010; Ruscheweyh *et al.* 2011). The mechanisms responsible for various forms of synaptic plasticity at the first sensory synapse are complex and not fully understood.

Presynaptic Ca^{2+} is the principal regulator of neurotransmitter release and synaptic plasticity that acts via multiple Ca^{2+}-sensing proteins to control almost every aspect of the synaptic vesicle life cycle. For example, Ca^{2+} triggers synchronous transmitter release via the low-affinity Ca^{2+} sensors synaptotagmins 1, 2 and 9 (Sugita *et al.* 2002; Xu *et al.* 2007), whereas asynchronous and spontaneous transmitter release are mediated by the high-affinity Ca^{2+} sensor Doc2 (Groffen *et al.* 2010; Yao *et al.* 2011). Endocytotic retrieval of synaptic vesicles is stimulated by Ca^{2+}/calcineurin-dependent dephosphorylation of dynamin-1 and other endocytotic proteins (Cousin & Robinson, 2001; Clayton & Cousin, 2009). Residual presynaptic $[Ca^{2+}]_i$ accumulated during repeated electrical stimulation contributes to short-term synaptic plasticity by controlling the size of the release-ready pool of synaptic vesicles (Zucker & Regehr, 2002; Neher & Sakaba, 2008) through Ca^{2+}-dependent activation of Munc13 and protein kinases A and C (PKA and PKC; Turner *et al.* 1999; Junge *et al.* 2004; Sørensen, 2004). To carry out these versatile synaptic functions, presynaptic Ca^{2+} signals must be precisely organized in time and space, which is achieved through the coordinated actions of Ca^{2+} channels, buffers and transporters. Therefore, identifying the specific components of presynaptic Ca^{2+} machinery is essential for understanding mechanisms of synaptic transmission and plasticity at any given synapse.

In spite of the key role of the first sensory synapse in transmitting sensory information and processing pain, the mechanisms that control presynaptic cytosolic Ca^{2+} concentration ($[Ca^{2+}]_i$) at this synapse are not known. Here we used cytosolic and mitochondrial Ca^{2+} imaging to examine mechanisms of presynaptic $[Ca^{2+}]_i$ clearance at the synapses formed between dorsal root ganglion (DRG) and spinal cord (SC) neurons in culture. We focused our analysis on a subset of nociceptive DRG neurons that express TRPV1 (transient receptor potential vanilloid 1) receptors because of their well-established role in acute and chronic pain (Caterina & Julius, 2001; Szallasi *et al.* 2007). Our data demonstrate that plasma membrane Ca^{2+}-ATPase (PMCA) and mitochondria are the major regulators of presynaptic $[Ca^{2+}]_i$ at this synapse.

Methods

Cell culture

DRG/SC co-cultures were prepared as previously described (Medvedeva *et al.* 2008, 2009). In brief, newborn (postnatal days 0–2) Sprague–Dawley rats were killed by decapitation with sharp scissors, according to a

protocol approved by the University of Iowa Institutional Animal Care and Use Committee and in accordance with the guidelines of the National Institutes of Health. Every effort was made to minimize the number of animals used. DRG were dissected from the thoracic and lumbar segments and incubated in pronase E dissolved in DMEM (1 mg ml^{-1}) containing 20 mM Hepes (pH 7.4) and penicillin–streptomycin (100 U ml^{-1} and 100 μg ml^{-1}, respectively) for 7 min at 37°C in a 10% CO_2 incubator. Ganglia were washed twice in cold DMEM containing Hepes (20 mM; pH 7.4) and then mechanically dissociated by trituration with flame-constricted Pasteur pipettes of decreasing diameter. The spinal cord was dissected into small segments (~0.5 mm) and then digested in DMEM containing 0.025% trypsin, Hepes (20 mM, pH 7.4) and penicillin–streptomycin (100 U ml^{-1} and 100 μg ml^{-1}, respectively) for 8 min at 37°C in a 10% CO_2 incubator. SC segments were then washed with cold complete DMEM medium supplemented with 5% heat-inactivated horse serum, 5% fetal bovine serum and penicillin–streptomycin (100 U ml^{-1} and 100 μg ml^{-1}, respectively) and dissociated using the procedure described above for DRG dissociation. Suspensions of SC and DRG cells were plated onto 25 mm glass coverslips coated with poly-L-ornithine and laminin. Cells were grown in DMEM supplemented with 5% heat-inactivated horse serum, 5% fetal bovine serum, insulin (6 μg ml^{-1}) and penicillin–streptomycin (100 U ml^{-1} and 100 μg ml^{-1}, respectively) in a 10% CO_2 incubator at 37°C. After 48 h, 5 μM cytosine β-D-arabinofuranoside (AraC) was added to cultures for 24 h. Two days later, cells were again treated with 5 μM AraC for 24 h. Cultures were grown for 10–16 days before use; 50% of the culture medium was replaced every 5–6 days.

Electrophysiological recordings

The methods for monitoring whole-cell Ca^{2+} currents and excitatory postsynaptic currents (EPSCs) were similar to those previously described by our group (Medvedeva *et al.* 2008, 2009). Whole-cell patch-clamp recordings were obtained using a Axopatch 200B patch-clamp amplifier and a Digidata 1322A analog-to-digital converter (Molecular Devices, Union City, CA, USA). Data were collected (filtered at 2 kHz and sampled at 5 kHz) and analysed using the pClamp 9 software (Molecular Devices). Patch pipettes were pulled from borosilicate glass (Narishige, New York, USA; 3–5 mΩ) on a Sutter Instruments (Novato, CA, USA) P-87 micropipette puller. For EPSC recordings, spinal cord neurons were voltage-clamped at –60 mV using patch pipettes that were filled with the following solution (mM): 125 potassium gluconate, 10 KCl, 3 Mg-ATP, 1 $MgCl_2$, 5 EGTA and 10 Hepes (pH 7.25 adjusted with KOH; 290 mosmol kg^{-1} with sucrose). The standard extracellular recording solution contained (mM): 140 NaCl, 5 KCl, 1.3 $CaCl_2$, 0.4 $MgSO_4$, 0.5 $MgCl_2$, 0.4 KH_2PO_4, 0.6 Na_2HPO_4, 3 $NaHCO_3$, 10 glucose and 10 Hepes (pH 7.4 with NaOH; 310 mosmol kg^{-1} with sucrose). The extracellular solution also contained 10 μM bicuculline and 2 μM strychnine to block inhibitory postsynaptic currents mediated by $GABA_A$ and glycine receptors, respectively. Evoked EPSCs in SC neurons were elicited every 4 s using a glass extracellular stimulating electrode (0.2–0.4 ms pulse) positioned near the cell body of a nearby DRG neuron. For Ca^{2+} current recordings, extracellular solution contained (mM): 115 choline chloride, 30 TEACl, 1.3 $CaCl_2$, 1 $MgCl_2$, 10 glucose, 10 Hepes and 1 μM tetrodotoxin (pH 7.4 with TEAOH; 310 mosmol kg^{-1} with sucrose); and the patch-pipette solution had the following composition (mM): 135 caesium gluconate, 3 Mg-ATP, 1 $MgCl_2$, 10 EGTA and 10 Hepes (pH 7.25 adjusted with CsOH; 290 mosmol kg^{-1} with sucrose). Voltage-gated Ca^{2+} currents were evoked by step depolarizations from –60 to +10 mV (100 ms, every 20 s).

Measurements of $[Ca^{2+}]_i$ in axonal boutons

The protocols for monitoring presynaptic $[Ca^{2+}]_i$ were similar to those we have previously described (Medvedeva *et al.* 2008, 2009). Cells were placed in a flow-through chamber mounted on the stage of an inverted IX-71 microscope (Olympus, Tokyo, Japan). For $[Ca^{2+}]_i$ measurements, DRG neurons were loaded with the low affinity (K_d ~ 5.5 μM) Ca^{2+} indicator Fura-FF (200 μM) or, in some experiments involving small-amplitude $[Ca^{2+}]_i$ measurements (see Figs 4*D*, *E* and 8*C*, *D*) the high-affinity (K_d = 225 nM) Ca^{2+} indicator Fura-2 (200 μM), via patch pipettes by holding neurons in the whole-cell configuration for 3–5 min; recordings began within 15–20 min of the pipette withdrawing. Only neurons that had membrane potential more negative than –50 mV immediately after patch membrane rupture were used for further experimentation. Fluorescence of Fura-FF or Fura-2 was alternately excited at 340 nm (12 nm bandpass) and 380 nm (12 nm) using a Polychrome IV monochromator (TILL Photonics, Gräfelfing, Germany) via a 40× oil-immersion objective (NA = 1.35, Olympus). Emitted fluorescence was collected at 510 (80) nm using an IMAGO CCD camera (TILL Photonics). Pairs of 340/380 nm images were sampled at 10 Hz. The fluorescence ratio ($R = F_{340}/F_{380}$) was converted to $[Ca^{2+}]_i$ according to the formula: $[Ca^{2+}]_i = K_d\beta(R - R_{min})/(R_{max} - R)$ (Grynkiewicz *et al.* 1985). The dissociation constants (K_d) used for Fura-2 and Fura-FF were 225 and 5500 nM, respectively (Molecular Probes Handbook). R_{min}, R_{max} and β were determined

by applying 10 μM ionomycin in Ca^{2+}-free buffer (1 mM EGTA) and saturating Ca^{2+} (1.3 mM Ca^{2+}). For Fura-2, calibration constants were: $R_{min} = 0.23$, $R_{max} = 2.70$ and $\beta = 4.75$. For Fura-FF, calibration constants were: $R_{min} = 0.21$, $R_{max} = 2.25$ and $\beta = 5.30$. Fluorescence was corrected for background, as determined prior to loading of cells with the indicators.

After dye loading and patch pipette withdrawal, intact DRG neurons were stimulated with trains of action potentials using extracellular field stimulation as previously described (Usachev & Thayer, 1999). In brief, field potentials were generated by passing current between two platinum electrodes via a Grass SS stimulator and a stimulus isolation unit (Quincy, MA, USA). Trains of 1 ms pulses were delivered at 10 Hz. The stimulus voltage threshold sufficient to elicit a detectable increase in $[Ca^{2+}]_i$ from neuronal processes and axonal boutons was determined before beginning an experiment, and the stimulus voltage for further experimentation was set at 20 V higher than the threshold voltage. An increase of the stimulus voltage above the threshold did not lead to a change in the amplitude of the resulting $[Ca^{2+}]_i$ transients. For the experiments involving substitution of intracellular K^+ with Cs^+ to examine the role of K^+-dependent Na^+/Ca^{2+} exchange (see Fig. 2*E*), DRG neurons were stimulated under the whole-cell voltage-clamp mode by applying 20 5-ms voltage pulses from a holding potential of –60 mV to +10 mV at a rate of 10 Hz.

Analysis of the rate of $[Ca^{2+}]_i$ clearance

The recovery phase of each $[Ca^{2+}]_i$ transient was fitted with a monoexponential function defined by the formula $[Ca^{2+}]_i = [Ca^{2+}]_{i0} + A\exp(-(t - t_0)/\tau)$ using a non-linear, least-squares curve fitting algorithm (Origin 7 software), where $[Ca^{2+}]_{i0}$ is the basal $[Ca^{2+}]_i$ level, A is the amplitude of the $[Ca^{2+}]_i$ response, t_0 is the time at the peak $[Ca^{2+}]_i$ and τ is the time constant describing $[Ca^{2+}]_i$ recovery. For a monoexponential $[Ca^{2+}]_i$ recovery process the rate of $[Ca^{2+}]_i$ clearance ($-d[Ca^{2+}]_i/dt$) is a linear function of $[Ca^{2+}]_i$ that can be determined by the formula: $-d[Ca^{2+}]_i/dt = k[Ca^{2+}]_i$, where the rate constant $k = 1/\tau$. To calculate the contribution of each specific Ca^{2+} transporting system, τ and k were calculated for each presynaptic $[Ca^{2+}]_i$ transient under control conditions ($\tau_{control}$, $k_{control}$) and after inhibition of the Ca^{2+} transporter ($\tau_{inhibit}$, $k_{inhibit}$) of interest. The rate constants were averaged, and the partial contribution of a specific Ca^{2+} transport was calculated as:

$$(k_{control} - k_{inhibit})/k_{control}100\%.$$

All the data are presented as mean ± SEM.

Measurements of mitochondrial Ca^{2+} concentrations ($[Ca^{2+}]_{mt}$) in axonal boutons

$[Ca^{2+}]_{mt}$ was measured using the mitochondria-targeted Ca^{2+} indicator mtPericam (Nagai *et al.* 2001) transferred to DRG neurons using lentivirus as previously described (Medvedeva *et al.* 2008). To visualize axonal boutons, DRG neurons overexpressing mtPericam were loaded with tetramethylrhodamine 10K dextran (Rhod10K; Invitrogen, Carlsbad, CA, USA) via patch pipettes (200 μM). mtPericam fluorescence was excited at 410 (12) nm via a 40× oil-immersion objective (NA = 1.35, Olympus) and measured at 530 (44) nm (sampling rate = 5 Hz). At 410 nm, a decrease in mtPericam fluorescence corresponds to the $[Ca^{2+}]_{mt}$ increase. $[Ca^{2+}]_{mt}$ changes were presented as

$$-\Delta F/F_0 = -(F - F_0)/F_0,$$

where F is the current fluorescence intensity and F_0 is the fluorescence intensity in the resting cell. The initial rate of $[Ca^{2+}]_{mt}$ increase was determined by dividing half of the $[Ca^{2+}]_{mt}$ amplitude by the time that was required to reach one half of $[Ca^{2+}]_{mt}$ peak.

Reagents

Fura-2, Fura-FF and Rhod10K were obtained from Invitrogen; capsaicin was from Tocris (Ellisville, MO, USA); ionomycin was from Calbiochem (San Diego, CA, USA); agatoxin IVA was from Bachem (Torrance, CA, USA); and ω-conotoxin GVIA was from Alomone Labs (Jerusalem, Israel). All other reagents were purchased from Sigma (St Louis, MO, USA).

RT-PCR analysis

Enriched neuronal DRG cultures were prepared as previously described (Usachev *et al.* 2002). In brief, DRG cultures were grown in the presence of AraC (5 μM) for 5–6 days to eliminate non-neuronal cells. To provide trophic support for this glial cell-deficient culture, fresh culture medium was mixed with an equal volume of medium conditioned by DRG cultures grown in the absence of AraC for 4–6 days. These growth conditions yield cultures containing ~75% of neurons and do not alter $[Ca^{2+}]_i$ homeostasis in DRG neurons (Usachev *et al.* 2002). Total RNA was isolated using the RNase easy mini kit (Qiagen, Valencia, CA, USA) and reverse transcribed and amplified using the one-step RT-PCR kit (Qiagen) according to the manufacturer's protocols. RT-PCR reactions were performed (Hybaid PCR Sprint Thermal Cycler, MA, USA) under the following conditions: 50°C for 30 min for reverse transcription, followed by 95°C for 15 min for initial PCR activation, then 30 cycles of 95°C for 1 min, 55°C for 1 min and 72°C for 1 min, and 72°C

Table 1. Primer sequences

Target gene (accession no.)	Primer sequence
NCX1	F: 5′-CTTCGTCCCACCTACAGAAT-3′
(NM_019268.2)	R: 5′-TGGTAGATGGCAGCAATGGA-3′
NCX2	F: 5′-TGCCATCCTGCTTTGACTAC-3′
(NM_078619.1)	R: 5′-GTCAACAGTGTGACCGAGAA-3′
NCX3	F: 5′-GAAACATGCAGCAGAGCAAG-3′
(NM_078620.1)	R: 5′-GACATTGCTCAGTCTCACGA-3′
NCKX1	F: 5′-CACCTTCCTGGGATCCATCATC-3′
(NM_020090.1)	R: 5′-CGATCTTCTAACATCACACTGATC-3′
NCKX2	F: 5′-TTATCATGTGGTGGGAAAGC-3′
(NM_031743.2)	R: 5′-GCTTTTTCTCTGAACCTCCC-3′
NCKX3	F: 5′-GACGTTTGCTTCCTCTACACTGT-3′
(NM_053505.1)	R: 5′-AACTCCGTCATGATGGAGAAA-3′
NCKX4	F: 5′-GGTGTGGCTGGTGACTATTATTG-3′
(NM_001108051.1)	R: 5′-CGTTGCTTCCGATGGTGTTAGAG-3′
NCKX5	F: 5′-CTTTCTCTAAGTTTACATGGTCTTAGT-C-3′
(NM_001107769.1)	R: 5′-CTTTCGGTCTAGTTTCCAGCC-G-3′
Letm1	F: 5′-AATAAGCTGCCCTCCACATTTG-3′
(NM_001005884.1)	R: 5′-TGTTTCAGCTGGCCCTTCAG-3′
NCLX	F: 5′-AGTCACCGCAGCCAAGTTCTT-C-3′
(NM_001017488.1)	R: 5′-AGTGCAGATGATGACCGTGACC-3′
MICU1	F: 5′-ACCCAATGAGAAGCAGCCAG-3′
(NM_199412.1)	R: 5′-ACGTCATGCTGCAGTTTACGC-3′
MCU	F: 5′-AGTACGGTTGTGCCCTCTGATG-3′
(NM_001106398.1)	R: 5′-AGTGGTCCTCTTCTCCGCTTTC-3′

for 10 min. Amplified transcripts were separated by electrophoresis on 1% agarose gels and detected using ethidium bromide. The sets of PCR primers are listed in Table 1.

Results

DRG neurons were co-cultured with spinal cord neurons for 10–16 days as previously described, to enable formation of sensory synapses *in vitro* (Medvedeva *et al.* 2008, 2009). Synapses formed by DRG and SC neurons grown in co-culture possess many important characteristics of the first sensory synapse, such as: (1) EPSCs are inhibited by the antagonists of 2-amino-3-(3-hydroxy-5-methyl-isoxazol-4-yl)propanoic acid (AMPA)-type glutamate receptors (Gruner & Silva, 1994; Gu & Macdermott, 1997; Bao *et al.* 1998; Medvedeva *et al.* 2008; Heinke *et al.* 2011); (2) N-type voltage-gated Ca^{2+} channels ($Ca_V2.2$) play the predominant role in controlling evoked glutamate release (Fig. 1*A* and *B*; Gruner & Silva, 1994; Bao *et al.* 1998; Heinke *et al.* 2004; Cao, 2006); (3) a large proportion of these synapses are sensitive to TRPV1 agonists such as capsaicin and NADA that produce dramatic increases in the frequency of spontaneous EPSCs (Fig. 1*C–E*; Yang *et al.* 1998; Huang *et al.* 2002; Sikand & Premkumar, 2007; Medvedeva *et al.*

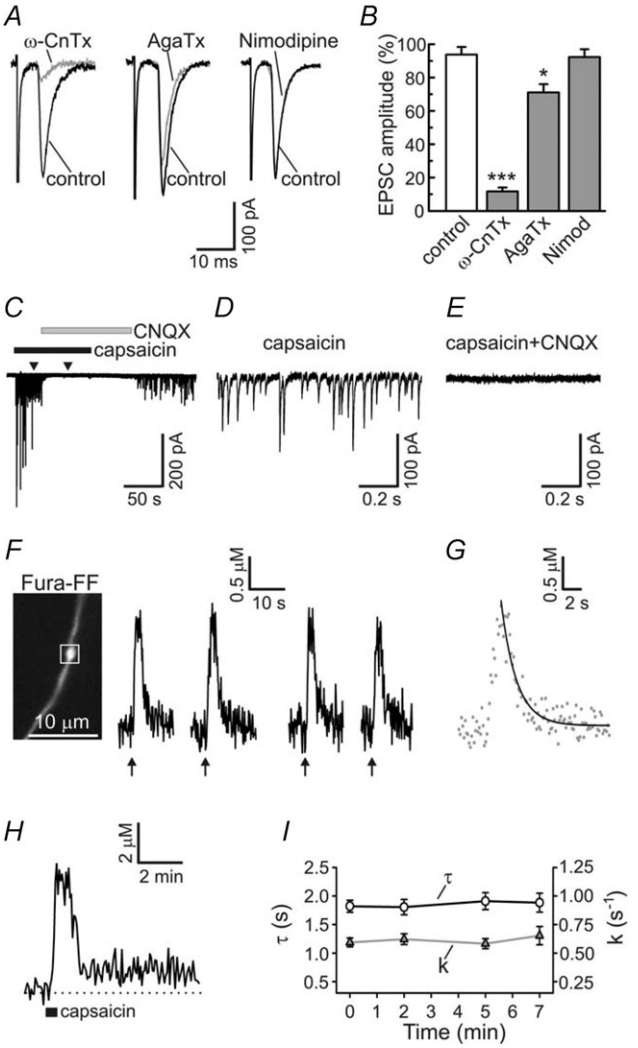

Figure 1. Characterization of synaptic transmission and action potential-evoked presynaptic $[Ca^{2+}]_i$ transients in DRG/SC co-culture

A, evoked EPSCs were recorded in DRG/SC co-culture as previously described (Medvedeva *et al.* 2008, 2009). The N-type voltage-gated Ca^{2+} channel (VGCC) inhibitor ω-conotoxin GVIA (1 μM; ω-CnTx) nearly completely abolished the EPSCs ($n = 7$), whereas the P/Q-type VGCC inhibitor agatoxin IVA (200 nM; AgaTx) produced a much smaller effect ($n = 5$). The EPSCs were not affected by the L-type VGCC inhibitor nimodipine (5 μM; $n = 7$). The superimposed EPSC traces represent recordings obtained before (control; black) and during the application of VGCC inhibitors (grey) for individual synaptic pairs. *B*, plot summarizing the effects of VGCC inhibitors (grey bars) or vehicle control (white bar) on EPSC amplitudes. To quantify the effects of VGCC inhibitors, 10 EPSC traces obtained in the presence of a given VGCC inhibitor (3 min of treatment) were averaged and normalized to the mean amplitude of the first 10 EPSC for each synaptic pair. $^*P < 0.05$, $^{***}P < 0.001$, one-way ANOVA with Dunnett's post test (relative to control). *C*, capsaicin (1 μM) strongly increases the frequency of spontaneous EPSCs. This effect is reversibly inhibited by the AMPA receptor antagonist CNQX (10 μM). Enhanced glutamate release continues long after the capsaicin washout as a result of prolonged mitochondria-dependent presynaptic $[Ca^{2+}]_i$ plateau (Medvedeva *et al.* 2008). *D* and *E*, two short segments of EPSC recordings from the experiment described in

2008); and (4) these synapses demonstrate wind-up and long-term potentiation (LTP)-like forms of synaptic plasticity (Vikman *et al.* 2001; Ji *et al.* 2003; Woolf & Salter, 2006). Consequently, the DRG/SC co-culture system has been widely used as a reliable tool for studying the first sensory synapse under highly defined recording conditions (Gu & Macdermott, 1997; Vikman *et al.* 2001; Tsuzuki *et al.* 2004; Sikand & Premkumar, 2007; Medvedeva *et al.* 2008, 2009).

$[Ca^{2+}]_i$ transients in presynaptic boutons of DRG neurons were measured using the low-affinity fluorescent Ca^{2+} indicator Fura-FF ($K_d \sim 5.5\,\mu M$). This dye is ideally suited for monitoring $[Ca^{2+}]_i$ changes predicted to be in the micromolar range, while the low Ca^{2+} affinity of the indicator minimizes its influence on Ca^{2+} buffering processes (Neher & Augustine, 1992). Fura-FF was loaded into small to medium-sized DRG neurons (18–32 μm) via a patch pipette, which enabled visualization of multiple axonal boutons along the processes (Figs 1–6). We have previously shown that these structures are associated with the presynaptic proteins synaptophysin and bassoon as well as the postsynaptic marker PSD95 (Medvedeva *et al.* 2008, 2009). $[Ca^{2+}]_i$ transients were evoked by a train of 20 action potentials applied at 10 Hz, consistent with firing patterns of primary sensory neurons *in vivo* (Meyer & Campbell, 1981; Slugg *et al.* 2000). Such stimulation produced $[Ca^{2+}]_i$ elevation from the basal level of $0.12 \pm 0.05\,\mu M$ to a peak of $2.14 \pm 0.12\,\mu M$ ($n = 79$ boutons/24 cells; Fig. 1*F*). After reaching its maximum, $[Ca^{2+}]_i$ rapidly recovered to the prestimulus level. For the majority of axonal boutons (79 of 84 tested), $[Ca^{2+}]_i$ recovery was well approximated using a monoexponential function with a time constant $\tau = 2.02 \pm 0.11$ s ($n = 79$ boutons/24 cells; Fig. 1*G*). Each cell was stimulated four times as described in Fig. 1*F*, and τ and the rate constant ($k = 1/\tau$) for each $[Ca^{2+}]_i$ transient were calculated. The first two stimuli were used as controls, and treatments directed at inhibiting various Ca^{2+} transporters were applied during the third and fourth stimuli. The contribution of a specific Ca^{2+} clearance mechanism was calculated as $(k_{control} - k_{inhibit})/k_{control}100\%$, where $k_{control}$ is the average rate constant in the control, and $k_{inhibit}$ is the average rate constant under conditions when a specific Ca^{2+} transporter is inhibited. In the absence of treatment, τ and k did not change significantly throughout the course of the experiment (Fig. 1*I*). Functional expression of TRPV1 was determined at the end of each experiment by applying 1 μM capsaicin (30 s; Fig. 1*H*), and only capsaicin-responding cells (mean presynaptic $[Ca^{2+}]_i$ elevation $\geq$ 100% above baseline) were used for further analysis. We used the described approach to determine the roles of plasma membrane Na^+/Ca^{2+} exchangers, PMCA, sarco-endoplasmic reticulum Ca^{2+}-ATPase (SERCA) and mitochondria in clearing Ca^{2+} from the presynaptic boutons of DRG neurons.

C are shown using an expanded time scale during the treatments with capsaicin alone (*D*) or capsaicin combined with CNQX (*E*). The times corresponding to these segments are shown by arrowheads in *C*. *F*, presynaptic $[Ca^{2+}]_i$ transients evoked by repeated trains of action potentials in capsaicin-sensitive DRG neurons. Presynaptic $[Ca^{2+}]_i$ transients were evoked by trains of action potentials (2 s at 10 Hz for each train; arrows) applied at the time points t = 0, 2, 5 and 7 min. Image on the left shows the distribution of Fura-FF fluorescence (λ_{ex} = 380 nm) in an unstimulated cell. $[Ca^{2+}]_i$ recording was made from the axonal bouton indicated by the white box. *G*, the second $[Ca^{2+}]_i$ transient from the experiment in *F* is shown on an expanded time scale (grey dots), and the monoexponential function obtained by fitting the recovery phase of this $[Ca^{2+}]_i$ transient is shown by a continuous line. *H*, $[Ca^{2+}]_i$ response to the TRPV1 agonist capsaicin (1 μM, 30 s), recorded from the axonal bouton in *F*. $[Ca^{2+}]_i$ rapidly recovered to a new steady-state level ($[Ca^{2+}]_i$ plateau), and remained elevated for an additional 5–15 min, as previously described (Medvedeva *et al.* 2008). *I*, summary of time constants (τ; open circles) and the rate constants (k; grey triangles) calculated for each presynaptic $[Ca^{2+}]_i$ transient, using the same experimental protocol as in *F*. Data are for 27 presynaptic boutons/6 cells. Time and rate constants did not change significantly during the time course of the experiments; repeated one-way ANOVA with Bonferroni post test.

Presynaptic Ca^{2+} clearance in DRG neurons depends to a small extent on plasma membrane Na^+/Ca^{2+} exchange

Plasma membrane Na^+/Ca^{2+} exchangers are low-affinity Ca^{2+} transporters that are expressed in excitable and non-excitable cells (Blaustein & Lederer, 1999; Lytton, 2007). Two large families of the exchangers have been identified: the K^+-independent Na^+/Ca^{2+} exchangers (NCX proteins), and the K^+ -dependent Na^+/Ca^{2+} exchangers (NCKX proteins). The NCX transporters utilize the transmembrane Na^+ gradient to extrude 1 Ca^{2+} ion from the cell in exchange for 3 or 4 Na^+ ions moved into the cell, whereas the NCKX transporters extrude 1 Ca^{2+} and 1 K^+ ion in exchange for 4 Na^+ ions (Blaustein & Lederer, 1999; Lytton, 2007). We blocked plasma membrane Na^+/Ca^{2+} exchange by replacing extracellular Na^+ with Li^+. This treatment produced a small but significant slowing of presynaptic $[Ca^{2+}]_i$ recovery (Fig. 2). In these experiments, the time constant of $[Ca^{2+}]_i$ recovery increased from 1.99 ± 0.24 s in control to 2.43 ± 0.31 s in Na^+-free external solution ($n = 15$ boutons/5 cells; $P < 0.05$, paired Student's t test). The corresponding rate constants were 0.59 ± 0.06 and $0.52 \pm 0.07\ s^{-1}$, respectively ($n = 15$ boutons/5 cells; $P < 0.05$, paired Student's t test). The overall contribution of plasma membrane Na^+/Ca^{2+} exchange to presynaptic Ca^{2+} clearance in DRG neurons was ~12%. Using the

high-affinity Ca^{2+} indicator Fura-2 we found that the Na^+/Ca^{2+} exchanger also controls presynaptic $[Ca^{2+}]_i$ at rest, as replacement of extracellular Na^+ with Li^+ resulted in a small but significant $[Ca^{2+}]_i$ elevation from 107 ± 4 to 134 ± 8 nM ($n = 20$ boutons/6 cells; $P < 0.001$, paired Student's t test; data not shown).

The NCX protein family comprises three isoforms (NCX1–3) and the NCKX family five (NCKX1–5). With the exception of NCKX1 (rod-specific isoform), all the NCX and NCKX isoforms are found in the brain (Annunziato *et al.* 2004; Lytton, 2007). DRG neurons express NCX2 and NCX3, whereas NCX1 is found primarily in satellite cells in the DRG (Persson *et al.* 2010). Which NCKX isoforms are expressed in DRG neurons is unknown. Using RT-PCR, we detected transcripts of NCX1, NCX2, NCX3 and NCKX2 in neuron-enriched DRG cultures (Fig. 2*D*). A very weak band corresponding to NCKX3 was also detected. Given the presence of some NCKX isoforms in DRG neurons, we examined whether presynaptic Ca^{2+} extrusion mediated by Na^+/Ca^{2+} exchange depends on K^+. Substitution of intracellular K^+ with Cs^+ inhibits NCKX2 and NCKX3 by 80 and 95%, respectively (Lee *et al.* 2007*b*). Therefore, we replaced K^+ with an equimolar amount of Cs^+ in the patch pipette solution (Fig. 2*E*). Since action potentials could not be evoked under these conditions, we stimulated the neurons by applying 20 short (5 ms) depolarization pulses (from –60 to +10 mV) at 10 Hz using the patch clamp technique. In the absence of intracellular K^+, the slowing of $[Ca^{2+}]_i$ recovery induced by Na^+ removal was similar to that observed in the presence of intracellular K^+ (compare graphs in Fig. 2*C* and *E*), suggesting that NCKX exchangers do not significantly contribute to Ca^{2+} clearance.

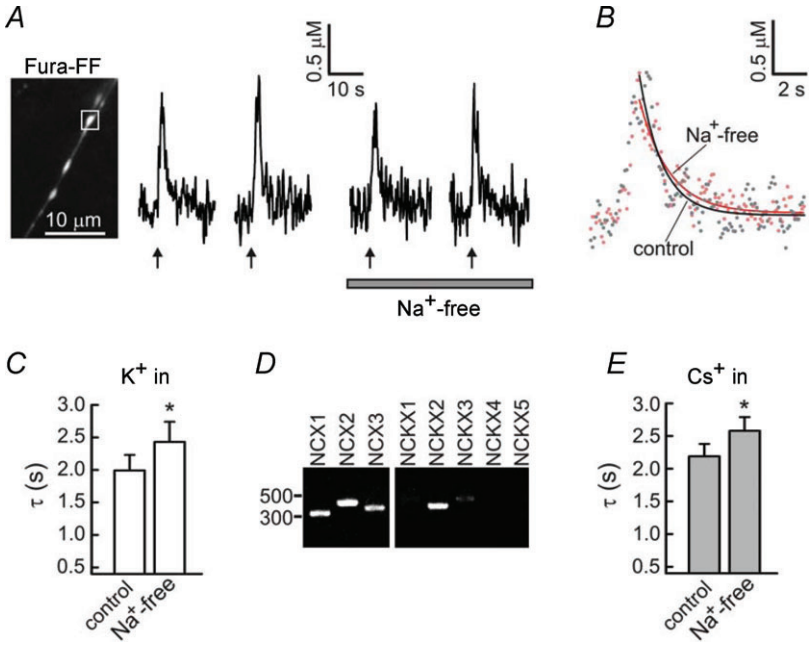

Figure 2. The rate of presynaptic $[Ca^{2+}]_i$ recovery is slightly reduced by inhibition of the plasma membrane Na^+/Ca^{2+} exchanger
A, $[Ca^{2+}]_i$ transients in an axonal bouton (white box) were evoked by trains of action potentials (20 action potentials at 10 Hz for each train; arrows) using extracellular field stimulation under control conditions and after equimolar substitution of extracellular Na^+ with Li^+ (Na^+-free). *B*, superimposition of $[Ca^{2+}]_i$ transients obtained under control (grey dots) and Na^+-free (red dots) conditions, for the axonal bouton in *A*. Continuous lines are the result of the monoexponential fitting procedure. *C*, summary of time constants (τ) describing presynaptic $[Ca^{2+}]_i$ recovery in control conditions and after substitution of extracellular Na^+ with Li^+ (Na^+-free). Experiments were performed as in *A*. The value of τ was calculated for each $[Ca^{2+}]_i$ transient. Time constants for the control condition were obtained by averaging τ for the first and second $[Ca^{2+}]_i$ transients, and those for the Na^+-free condition were obtained by averaging τ for the third and fourth $[Ca^{2+}]_i$ transients. $^*P < 0.05$; paired Student's t test; $n = 15$ boutons/5 cells *D*, RT-PCR analysis of NCX1–3 and NCKX1–5 expression in neuron-enriched rat DRG culture. *E*, summary of time constants describing presynaptic $[Ca^{2+}]_i$ recovery obtained under control and Na^+-free (equimolar substitution with Li^+) conditions in the absence of intracellular K^+ (equimolar substitution with Cs^+ in the patch pipette). The experimental protocol was similar to that described in *A*, except that the cells were stimulated under the whole-cell mode of patch-clamp (voltage-clamp), by 20 voltage steps from –60 to +10 mV, for 5 ms each and applied at 10 Hz. The control time constants were obtained by averaging τ for the first and second $[Ca^{2+}]_i$ transients, and the Na^+-free time constants were obtained by averaging τ for the third and fourth $[Ca^{2+}]_i$ transients. $^*P < 0.05$, paired Student's t test.

Presynaptic Ca^{2+} clearance in DRG neurons is highly dependent on PMCA

PMCAs are key components of Ca^{2+} extrusion in central and peripheral neurons (Benham *et al.* 1992; Usachev *et al.* 2002; Wanaverbecq *et al.* 2003; Empson *et al.* 2007; Gover *et al.* 2007*b*). Four major PMCA isoforms (1–4) have been identified (Carafoli, 1991; Strehler & Zacharias, 2001), and we previously showed that PMCA2 and PMCA4 are the major isoforms expressed in DRG neurons (Usachev *et al.* 2002). In addition, strong PMCA4 immunoreactivity was detected in the superficial layers of the dorsal horn (Tachibana *et al.* 2004), the area where the majority of TRPV1-positive central processes terminate (Guo *et al.* 1999; Cavanaugh *et al.* 2011). Here we examined the functional significance of PMCAs in presynaptic boutons of DRG neurons. Ca^{2+} extrusion by PMCA requires the countertransport of protons, and thus can be blocked by raising extracellular pH (Carafoli, 1991; Schwiening *et al.* 1993; Usachev *et al.* 2002; Wanaverbecq *et al.* 2003). Using Fura-2, we found that blocking PMCA by raising extracellular pH to 8.8 led to baseline $[Ca^{2+}]_i$ elevation from 98 ± 5 to 178 ± 12 nM ($n = 29$ boutons/6 cells; $P < 0.001$, Student's t test; data not shown). Fura-FF-based measurements determined that PMCA inhibition markedly slowed $[Ca^{2+}]_i$ recovery in the axonal boutons of DRG neurons (Fig. 3). The time constant increased from 2.01 ± 0.19 s in control to 4.29 ± 0.53 s at pH 8.8 ($n = 27$ boutons/7 cells; $P < 0.001$, paired Student's t test). The corresponding rate constants were 0.60 ± 0.06 and 0.32 ± 0.03 s^{-1}, respectively ($n = 27$ boutons/7 cells; $P < 0.001$, paired Student's t test). The contribution of PMCA to presynaptic $[Ca^{2+}]_i$ clearance was ~47%.

We also found that PMCA blockade resulted in a mild but significant increase of the amplitude of electrically evoked presynaptic $[Ca^{2+}]_i$ responses from 1.83 ± 0.14 μM in control to 2.25 ± 0.19 μM at pH 8.8 ($n = 27$ boutons/7 cells; $P < 0.01$, paired Student's t test). Raising extracellular pH to 8.8 did not have any significant effect on voltage-gated Ca^{2+} currents in DRG neurons, as determined by whole-cell patch-clamp recordings (Fig. 3*D*). Thus, PMCA strongly contributes to multiple aspects of presynaptic $[Ca^{2+}]_i$ signalling in DRG neurons, including maintenance of low $[Ca^{2+}]_i$ at rest, regulation of the $[Ca^{2+}]_i$ clearance rate and setting the amplitude of $[Ca^{2+}]_i$ elevation in response to action potentials.

Presynaptic Ca^{2+} clearance does not depend on SERCA

SERCA is a high-affinity Ca^{2+} pump that serves to lower cytosolic Ca^{2+} and replenish intracellular Ca^{2+} stores for subsequent Ca^{2+} release via the ryanodine or inositol 1,4,5-trisphosphate (IP_3) receptors (Henzi & MacDermott, 1992; Pozzan *et al.* 1994; Thomas & Hanley, 1994). Three SERCA isoforms (1–3) have been identified, two of which (SERCA2 and SERCA3) are present in the brain (Mata & Sepulveda, 2005; Vangheluwe *et al.* 2009). SERCA plays an important role in regulating $[Ca^{2+}]_i$ in the somata of DRG and trigeminal neurons,

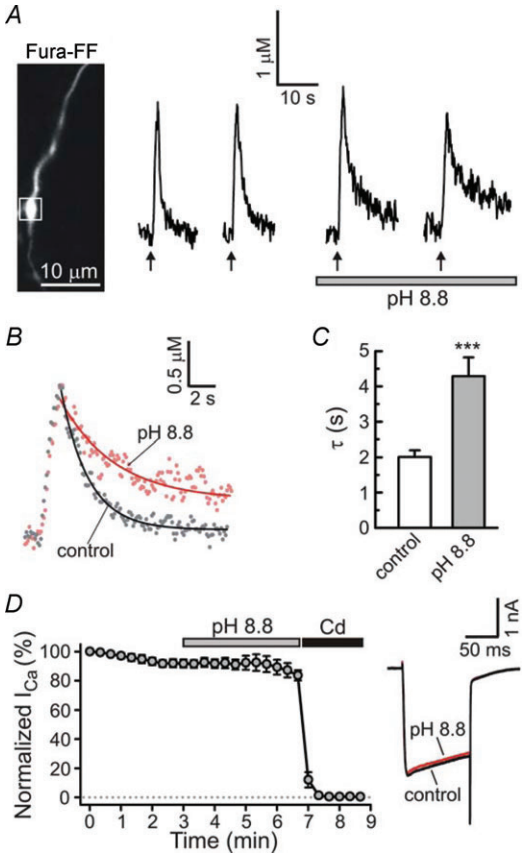

Figure 3. The rate of presynaptic $[Ca^{2+}]_i$ recovery is markedly slowed by inhibition of PMCA
A, $[Ca^{2+}]_i$ transients were evoked by trains of 20 action potentials at 10 Hz (arrows) using extracellular field stimulation under control conditions and after raising extracellular pH to 8.8 to block PMCA. The white box indicates an axonal bouton from which $[Ca^{2+}]_i$ traces were recorded. *B*, superimposition of control $[Ca^{2+}]_i$ (grey dots) with that obtained under conditions of elevated extracellular pH (red dots). Continuous lines show the results of monoexponential fitting procedure for the corresponding traces. *C*, plot summarizing τ obtained from seven independent experiments similar to that shown in *A*. Control time constants were obtained by averaging τ for the first and second $[Ca^{2+}]_i$ responses, and the time constants for pH = 8.8 were obtained by averaging τ for the third and fourth $[Ca^{2+}]_i$ responses. ***$P < 0.001$, paired Student's t test, $n = 27$ boutons/7 cells. *D*, raising extracellular pH to 8.8 does not affect the amplitude of voltage-activated Ca^{2+} currents (I_{Ca}). Plot (left) summarizing I_{Ca} recordings (100 ms depolarizations from –60 to +10 mV) in DRG neurons ($n = 6$) in control and following treatments with either pH 8.8 or a blocker of voltage-gated Ca^{2+} channels, Cd^{2+} (500 μM). The I_{Ca} amplitudes were normalized to the amplitude of the first I_{Ca} response recorded for each cell. The right panel shows a superimposition of representative I_{Ca} traces in control conditions (black) and following extracellular pH increase to 8.8 (red).

and its contribution to $[Ca^{2+}]_i$ clearance can be 50% and higher, depending on the stimulation protocol and sensory neuron population (Shmigol *et al.* 1994; Usachev & Thayer, 1999; Lu *et al.* 2006; Gover *et al.* 2007*a*). We tested the effects of a selective SERCA inhibitor, cyclopiazonic acid (CPA, 5 μM), on $[Ca^{2+}]_i$ in the presynaptic boutons of DRG neurons. Application of 5 μM CPA did not affect the recovery kinetics of presynaptic $[Ca^{2+}]_i$ transients (Fig. 4*A*–*C*), and the time constants were 1.97 ± 0.27 and 2.21 ± 0.31 s in control and in the presence of CPA, respectively ($n = 18$ boutons/5 cells; $P = 0.28$, paired Student's t test). The corresponding rate constants were 0.66 ± 0.08 and $0.62 \pm 0.09\ s^{-1}$, respectively ($P = 0.39$, paired Student's t test). Similar results were obtained using another SERCA inhibitor, thapsigargin (Tg) (Thomas & Hanley, 1994; Thayer *et al.* 2002). Treatment with 1 μM Tg did not significantly change the time constant, which was 2.18 ± 0.17 s in the absence and 2.13 ± 0.19 s in the presence of 1 μM Tg ($n = 16$ boutons/4 cells; $P = 0.72$, paired Student's t test; data not shown). Thus, Ca^{2+} clearance in the presynaptic boutons of DRG neurons is independent of SERCA.

To test whether functional endoplasmic reticulum (ER) Ca^{2+} stores are present in the axonal boutons of DRG neurons, we applied an activator of Ca^{2+} release from ryanodine-sensitive stores, caffeine, in a Ca^{2+}-free buffer. To improve the detection of potentially small $[Ca^{2+}]_i$ changes in response to caffeine, we used a high-affinity Ca^{2+} indicator, Fura-2 ($K_d = 225$ nM), in these experiments. Application of 10 mM caffeine produced a small but detectable Ca^{2+} release in presynaptic boutons with an amplitude of 76 ± 11 nM ($n = 27$ boutons/5 cells; Fig. 4*D* and *E*). This value was significantly smaller than that for the caffeine-induced $[Ca^{2+}]_i$ responses in the somata of DRG neurons (159 ± 39 nM; $n = 5$; $P < 0.01$, non-paired Student's t test). In contrast, $[Ca^{2+}]_i$ transients induced by electrical stimulation were larger in the axonal boutons than those in the somata (Fig. 4*D*; arrow). Notably, after caffeine-induced depletion of the ER Ca^{2+} stores, switching from a Ca^{2+}-free to normal solution containing 1.3 mM Ca^{2+} led to a pronounced $[Ca^{2+}]_i$ overshoot in both presynaptic boutons and somata. This transient $[Ca^{2+}]_i$ elevation is probably the result of activation of store-operated Ca^{2+} channels, as previously described for DRG neurons (Usachev & Thayer, 1999; Lu *et al.* 2006; Gemes *et al.* 2011). Moreover, depleting Ca^{2+} stores with 5 μM CPA or 1 μM Tg induced small but

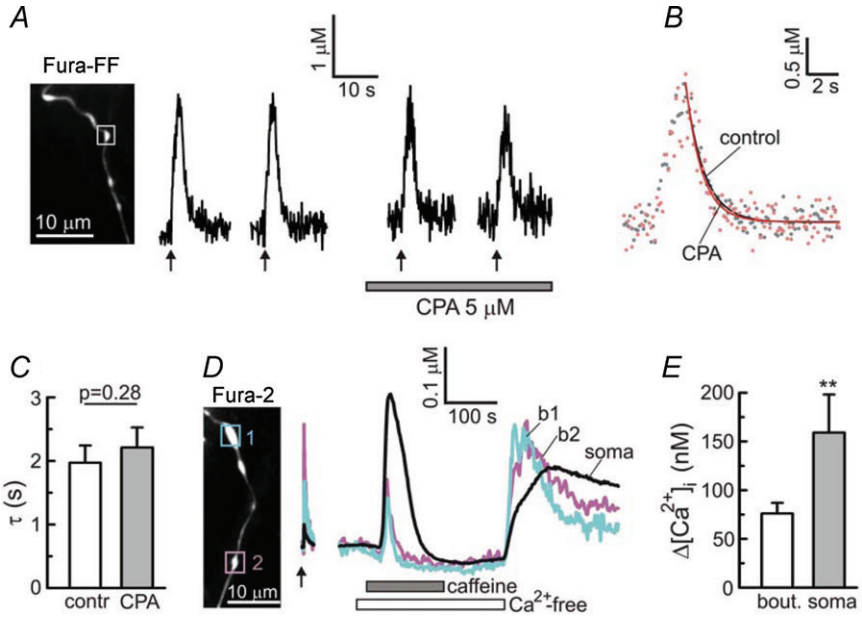

Figure 4. The rate of presynaptic Ca^{2+} clearance is not affected by inhibition of SERCA
A, $[Ca^{2+}]_i$ transients in axonal bouton (white box) were evoked by trains of action potentials (10 Hz for 2 s) in the absence or presence (5 μM) of the SERCA inhibitor cyclopiazonic acid (CPA). The CPA treatment started 3 min prior to the third stimulation. *B*, $[Ca^{2+}]_i$ transients generated in the absence (grey dots) or presence of 5 μM CPA (red dots) are superimposed. The $[Ca^{2+}]_i$ traces were offset along the *y*-axis to facilitate comparison. Traces obtained by monoexponential fitting of the corresponding $[Ca^{2+}]_i$ data points are shown by continuous lines. *C*, plot summarizing time constants for $[Ca^{2+}]_i$ recovery in controls (contr) and in the presence of 5 μM CPA (paired Student's t test, $n = 18$ boutons/4 cells). *D*, $[Ca^{2+}]_i$ changes recorded from two axonal boutons (b1 and b2, squares) and the cell body of a Fura-2-loaded DRG neuron in response to electrical stimulation (6 Hz for 5 s; arrow) or the ryanodine receptor activator caffeine (10 mM). *E*, comparison of the amplitudes of $[Ca^{2+}]_i$ responses to 10 mM caffeine in axonal boutons ($n = 27$ boutons/5 cells) and somata ($n = 5$) of DRG neurons. $^{**}P < 0.01$, unpaired Student's t test.

significant presynaptic $[Ca^{2+}]_i$ elevations from 106 ± 3 to 152 ± 5 nM for CPA ($n = 38$ boutons/7 cells; $P < 0.001$ paired Student's t test) and from 116 ± 8 to 134 ± 7 nM for Tg ($n = 14$ boutons/4 cells; $P < 0.001$ paired Student's t test), consistent with the functional presence of store-operated Ca^{2+} channels in presynaptic boutons of DRG neurons.

Mitochondria regulate the amplitude and duration of presynaptic $[Ca^{2+}]_i$ transients in DRG neurons

Presynaptic terminals and boutons are densely packed with mitochondria that support high energy demand at the synapses (Hollenbeck, 2005; Ly & Verstreken, 2006). Mitochondria also contribute to presynaptic Ca^{2+} signalling and synaptic plasticity at several central synapses, as well as at the neuromuscular junction (Billups & Forsythe, 2002; David & Barrett, 2003; Jonas, 2004; Garcia-Chacon *et al.* 2006; Lee *et al.* 2007*a*). We recently reported that mitochondria control TRPV1-mediated prolonged elevations of presynaptic $[Ca^{2+}]_i$ and glutamate release at the first sensory synapse (Medvedeva *et al.* 2008). Here we examined whether mitochondria are also involved in shaping presynaptic $[Ca^{2+}]_i$ transients in response to brief trains of action potentials. Ca^{2+} uptake by mitochondria is mediated by the mitochondrial Ca^{2+} uniporter (MCU), and the mitochondrial membrane potential $\Delta\Psi_{mt}$ (~ –150 mV) provides the driving force for the Ca^{2+} uptake (Bernardi, 1999; Nicholls & Budd, 2000; Thayer *et al.* 2002). Mitochondrial Ca^{2+} uptake can be blocked by depolarizing mitochondria with a protonophore, carbonyl cyanide *p*-trifluoromethoxyphenylhydrazone (FCCP). We examined the effects of 1 μM FCCP on presynaptic $[Ca^{2+}]_i$ transients induced by electrical stimulation (10 Hz for 2 s). FCCP treatment was combined with application of the F_1,F_0 ATP-synthase inhibitor oligomycin (2 μM) to prevent ATP depletion via the reverse mode of the synthase (Nicholls & Ward, 2000; Toescu & Verkhratsky, 2003). Using Fura-2, we found that FCCP+oligomycin increased baseline presynaptic $[Ca^{2+}]_i$ from 126 ± 6 to 163 ± 7 nM ($n = 17$ boutons/4 cells; $P < 0.001$ Student's t test). Fura-FF-based measurements revealed that FCCP produced a marked slowing of $[Ca^{2+}]_i$ recovery in the axonal boutons of DRG neurons (Fig. 5). The time constants were 2.11 ± 0.21 s in control and 4.60 ± 0.39 s after the FCCP treatment ($n = 17$ boutons/5 cells; $P < 0.001$, paired Student's t test). The corresponding rate constants were 0.54 ± 0.05 and 0.25 ± 0.02 s^{-1}, respectively ($n = 17$ boutons/5 cells; $P < 0.001$, paired Student's t test). We also found that the amplitudes of the $[Ca^{2+}]_i$ responses increased from 2.17 ± 0.24 μM in control to 3.45 ± 0.42 μM in the presence of FCCP ($n = 17$ boutons/5 cells; $P < 0.01$, paired Student's t test). Whole-cell patch-clamp recordings showed that FCCP+oligomycin treatment reduced voltage-gated Ca^{2+} currents by ~30% in DRG neurons (Fig. 5*D*), probably as a result of reduced Ca^{2+} buffering and, consequently, increased Ca^{2+}-dependent inhibition of voltage-gated Ca^{2+} channels (Hernandez-Guijo *et al.* 2001). Overall, our data suggest that mitochondria play

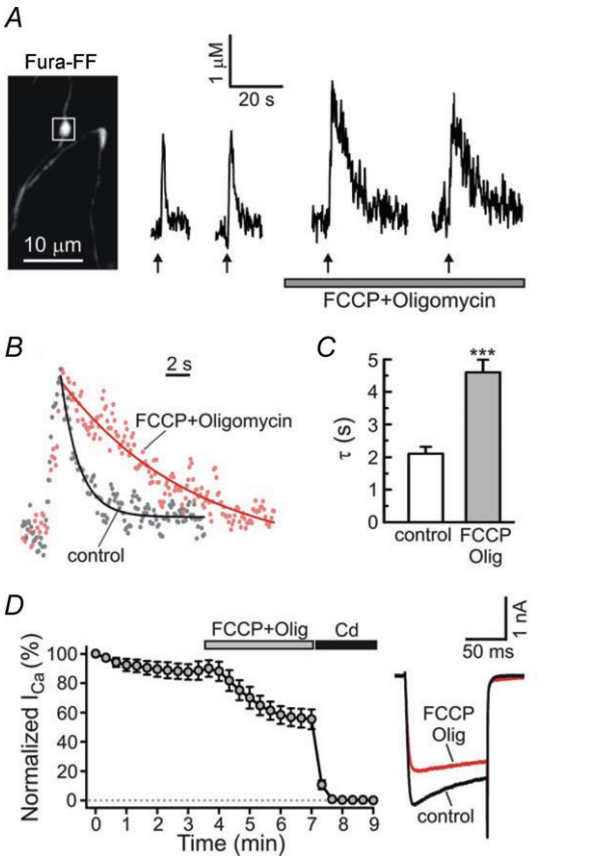

Figure 5. Inhibition of mitochondrial uptake by FCCP strongly reduces the rate of presynaptic Ca^{2+} clearance
A, electrically evoked $[Ca^{2+}]_i$ transients (10 Hz, 2 s; arrows) were recorded from axonal boutons of capsaicin-sensitive DRG neurons (image on the left) in control and during treatment with the mitochondrial protonophore FCCP (1 μM) and F1,Fo ATP-synthase inhibitor oligomycin B (2 μM). *B*, superimposition of $[Ca^{2+}]_i$ traces in control (grey dots; second trace in *A*) conditions and in the presence of 1 μM FCCP + 2 μM oligomycin (red dots; third trace in *A*). Plots obtained by monoexponential fitting of $[Ca^{2+}]_i$ recovery are shown by continuous lines. *C*, plot summarizing the time constant data for all the experiments as those shown in *A*. ***$P < 0.001$, paired Student's t test. *D*, treatment with 1 μM FCCP + 2 μM oligomycin decreased the amplitude of voltage-activated Ca^{2+} currents (I_{Ca}) in DRG neurons. Amplitudes of I_{Ca} (depolarization from –60 to +10 mV for 100 ms) were normalized to the amplitude of the first evoked I_{Ca} for each cell ($n = 5$). The effect of FCCP + oligomycin was significant starting from $t = 5$ min ($P < 0.001$; repeated one-way ANOVA with Dunnett's post test relative to control I_{Ca} taken at $t = 3$ min). I_{Ca} was completely blocked by 500 μM Cd^{2+}. Plot on the right shows superimposition of representative I_{Ca} traces in control conditions (black) and after 2 min of treatment using FCCP + oligomycin (red).

an important role in buffering presynaptic Ca^{2+} influx and clearing $[Ca^{2+}]_i$ elevations after periods of neuronal activity.

MCU-mediated Ca^{2+} transport can be blocked directly by ruthenium red (RuR; Bernardi, 1999; Thayer *et al.* 2002). An important advantage of this approach is that it does not disrupt either the mitochondrial electrochemical gradient or the $\Delta\Psi_{mt}$. RuR is membrane impermeable and thus was delivered to the cell through a patch pipette (10 μM) along with Fura-FF (see Methods). The amplitudes of action potential-evoked $[Ca^{2+}]_i$ transients were significantly larger in RuR-loaded boutons (4.63 ± 0.45 μM; 33 boutons/7 cells) than in control cells (2.02 ± 0.12 μM; 79 boutons/24 cells; $P < 0.001$, unpaired Student's t test). As shown in Fig. 6, treatment with RuR also led to a marked slowing of presynaptic $[Ca^{2+}]_i$ recovery. The time constants were 2.06 ± 0.10 s in control cells ($n = 79$ boutons/24 cells) and 3.35 ± 0.16 s in RuR-treated cells ($n = 33$ boutons/7 cells; $P < 0.001$, unpaired Student's t test). The corresponding rate constants were $0.58 \pm 0.03\ s^{-1}$ in control cells ($n = 79$ boutons/24 cells) and $0.35 \pm 0.02\ s^{-1}$ in RuR-loaded cells ($n = 33$ boutons/7 cells; $P < 0.001$, unpaired Student's t test). Thus, mitochondria blunt presynaptic $[Ca^{2+}]_i$ elevations and play important role in presynaptic Ca^{2+} clearance in DRG neurons. The mitochondrial contribution to $[Ca^{2+}]_i$ recovery process ranges between 40% (based on RuR experiments) and 54% (based on FCCP experiments).

It has been proposed that the Ca^{2+} accumulated in mitochondria can stimulate several Ca^{2+}-dependent dehydrogenases and thereby enhance the production of ATP (Hajnoczky *et al.* 1995; Denton, 2009). Thus, the inhibition of mitochondrial Ca^{2+} uptake could potentially slow ATP-dependent transport, such as PMCA-mediated Ca^{2+} efflux. We therefore tested the role of PMCA in RuR-treated neurons. Inhibiting PMCA by raising extracellular pH to 8.8 produced a more than two-fold increase in the time constant, from 3.44 ± 0.20 s in RuR only-treated cells to 7.80 ± 0.53 s after a combined RuR + pH 8.8 treatment ($n = 16$ boutons/5 cells; $P < 0.001$, paired Student's t test;

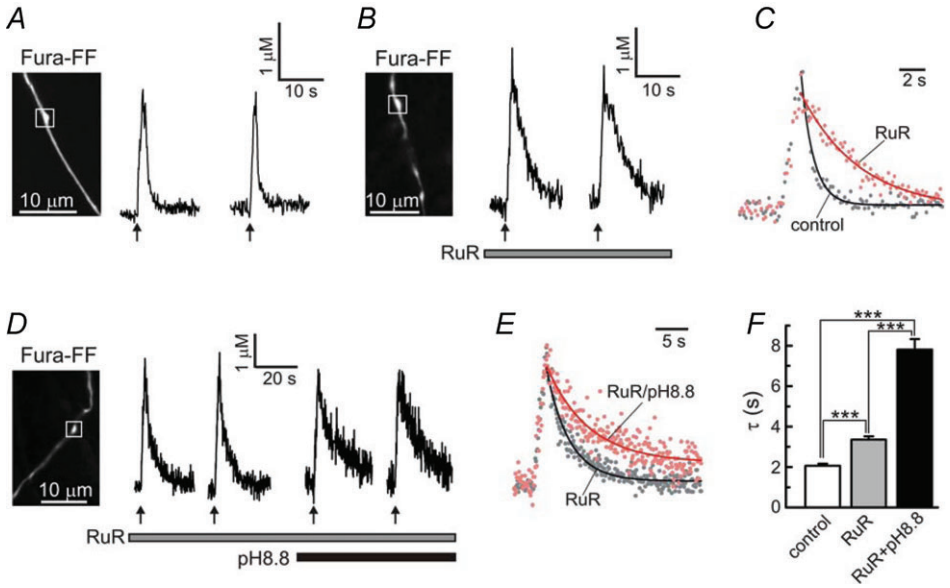

Figure 6. The rate of presynaptic $[Ca^{2+}]_i$ recovery is significantly reduced by inhibition of the mitochondrial uniporter
A and *B*, action potential-evoked (10 Hz for 2 s; arrows) $[Ca^{2+}]_i$ transients were recorded in control cells (*A*) and cells loaded with the MCU inhibitor ruthenium red (RuR; *B*). In the latter case, 10 μM RuR was included in the patch pipette solution, along with 200 μM Fura-FF. White boxes indicate axonal boutons from which recordings were made. *C*, control $[Ca^{2+}]_i$ trace (grey dots) is superimposed with a $[Ca^{2+}]_i$ trace recorded in the presence of 10 μM RuR (red dots). $[Ca^{2+}]_i$ transients were normalized to facilitate comparison of the recovery kinetics. Continuous lines indicate the plots obtained by monoexponential fitting of the corresponding $[Ca^{2+}]_i$ traces. *D*, $[Ca^{2+}]_i$ transients were studied in cells containing 10 μM RuR under normal (pH = 7.4) or basic (pH = 8.8) extracellular pH. $[Ca^{2+}]_i$ responses were induced by trains of action potentials (10 Hz for 2 s, arrows) generated by extracellular field stimulation. *E*, superimposition of $[Ca^{2+}]_i$ transients obtained under normal (pH = 7.4; grey dots) or elevated (pH = 8.8) extracellular pH (red dots), for the same cell as shown in *D*. Continuous lines represent mononexponential fitting of the corresponding $[Ca^{2+}]_i$ data points. *F*, summary of the effects of RuR and high pH on the time constant of $[Ca^{2+}]_i$ recovery. The data were obtained from experiments such as those shown in *A*, *B* and *D*. ***$P < 0.001$, one-way ANOVA with Bonferroni post test; $n = 79$ boutons/24 cells for control; $n = 33$ boutons/7 cells for RuR only; $n = 16$ boutons/5 cells for RuR + pH 8.8.

Fig. 6*D-F*). The magnitude of the pH 8.8 effect in RuR-treated cells was similar to the pH 8.8 effect in control cells (Fig. 3), indicating that PMCA-mediated Ca^{2+} transport was independent of the RuR-sensitive mitochondrial Ca^{2+} uptake under the described experimental conditions. We were unable to perform similar experiments in FCCP-treated cells because the combined application of FCCP and pH 8.8 destabilized presynaptic $[Ca^{2+}]_i$ in DRG neurons ($n = 14$ boutons/3 cells; data not shown).

Properties of Ca^{2+} uptake by presynaptic mitochondria in DRG neurons

Given that mitochondria significantly contribute to the amplitude and time course of changes in presynaptic $[Ca^{2+}]_i$, we next examined the properties of Ca^{2+} transport by presynaptic mitochondria in capsaicin-sensitive DRG neurons. In these experiments, we directly monitored $[Ca^{2+}]_{mt}$ using a mitochondria-targeted Ca^{2+} indicator, mtPericam (Nagai *et al.* 2001), as previously described (Medvedeva *et al.* 2008). DRG neurons transfected with mtPericam were subsequently loaded with Rhod10K through a patch pipette to enable visualization of axonal varicosities (Fig. 7*A*). Stimulating DRG neurons with trains of action potentials produced a rapid $[Ca^{2+}]_{mt}$ elevation. Only 3–5 action potentials were required to produce detectable Ca^{2+} uptake by mitochondria (Fig. 7*B*). Comparison of the time courses of $[Ca^{2+}]_i$ and $[Ca^{2+}]_{mt}$ showed that mitochondrial Ca^{2+} uptake developed with a 1–2 s delay relative to the presynaptic $[Ca^{2+}]_i$ rise. For example, in response to a stimulus with 20 action potentials (10 Hz, 2 s), $[Ca^{2+}]_i$ and $[Ca^{2+}]_{mt}$ reached their peak values within 1.9 ± 0.1 s (79 boutons/24 cells) and 3.5 ± 0.2 s ($n = 22$ boutons/5 cells; $P < 0.001$, unpaired Student's *t* test compared to the $[Ca^{2+}]_i$ rising time) after beginning of the stimulation, respectively. In addition, Ca^{2+} removal from mitochondria occurred at a markedly slower rate (half recovery time $= 9.2 \pm 0.8$ s; $n = 22$ boutons/5 cells) than Ca^{2+} clearance from the presynaptic cytosol (Fig. 7*D*). The fact that $[Ca^{2+}]_{mt}$ remained elevated long after $[Ca^{2+}]_i$ has fully recovered suggests that mitochondria serve as an integrator of consecutive presynaptic $[Ca^{2+}]_i$ spikes produced by repeated neuronal stimulation.

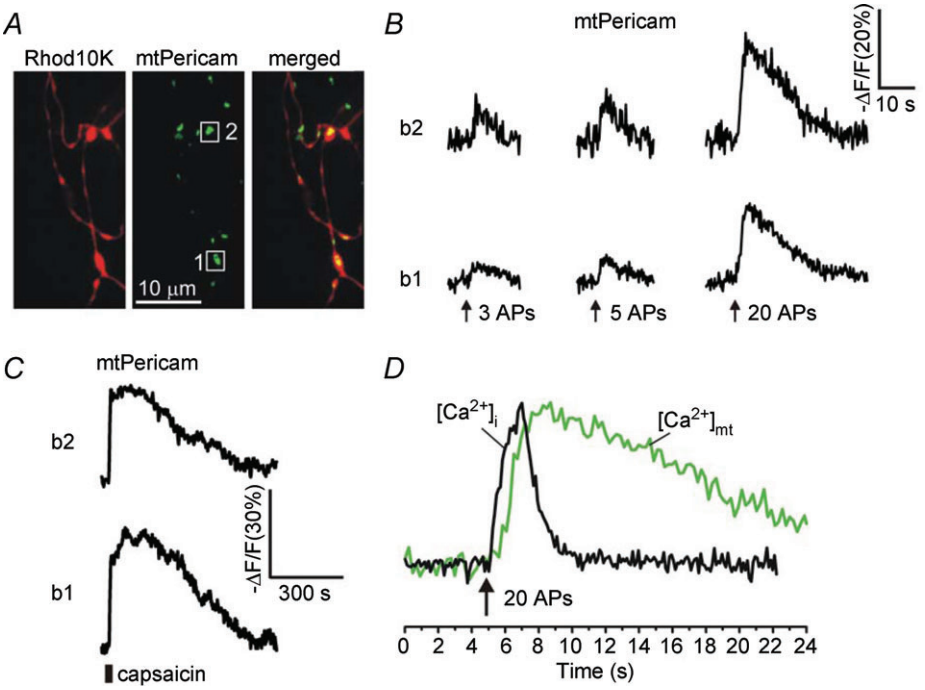

Figure 7. Ca^{2+} changes in presynaptic mitochondria ($[Ca^{2+}]_{mt}$) monitored using mitochondria-targeted Ca^{2+} indicator mtPericam
A, DRG neurons were transfected with mtPericam (green) and subsequently loaded with rhodamine 10K dextran (Rhod10K; 200 μM; red) via a patch pipette to facilitate the visualization of axonal boutons. *B*, mitochondrial Ca^{2+} changes were evoked by 3, 5 or 20 action potentials (10 Hz) and recorded from two axonal boutons (b1 and b2) indicated by white boxes in *A*. *C*, $[Ca^{2+}]_{mt}$ responses to 1 μM capsaicin (30 s) for the same axonal boutons as in *B*. *D*, comparison of typical $[Ca^{2+}]_i$ (black) and $[Ca^{2+}]_{mt}$ (green) changes induced by 20 action potentials (10 Hz for 2 s). The $[Ca^{2+}]_{mt}$ trace was obtained by averaging traces from five axonal boutons of the cell depicted in *A*. The $[Ca^{2+}]_i$ trace was generated by averaging traces from four axonal boutons of a different cell loaded with Fura-FF. The traces were normalized along the vertical axis.

Next we addressed the important and widely debated question of how mitochondrial Ca^{2+} uptake depends on $[Ca^{2+}]_i$. The reported values for the Ca^{2+} affinity of MCU cover a wide range (0.5–20 μM), depending on the preparation, cell type and method of monitoring mitochondrial Ca^{2+} uptake (Gunter & Pfeiffer, 1990; Bernardi, 1999; Spat *et al.* 2008). In neuronal preparations, high Ca^{2+} sensitivity of MCU ($K_{0.5}$ ~0.4–0.5 μM) was reported for presynaptic mitochondria at nerve–muscular junctions of the fruit-fly and lizard (David, 1999; Chouhan *et al.* 2010). In contrast, mitochondrial Ca^{2+} uptake in the cell body of bullfrog sympathetic neurons was estimated to have a much lower Ca^{2+} affinity ($K_{0.5}$ ~ 10 μM; Colegrove *et al.* 2000). Comparable quantifications in mammalian neurons are lacking. To determine the dependence of mitochondrial Ca^{2+} uptake on $[Ca^{2+}]_i$ in axonal boutons of DRG neurons, we compared $[Ca^{2+}]_i$ and $[Ca^{2+}]_{mt}$ elevations induced by depolarizing pulses of incremental amplitude (extracellular buffers containing 10, 15, 20, 30, 50 or 90 mM KCl; Fig. 8), as well as by treating cells with 1 μM capsaicin, which is known to produce large presynaptic $[Ca^{2+}]_i$ and $[Ca^{2+}]_{mt}$ elevations in DRG neurons (Medvedeva *et al.* 2008). To facilitate detection of small presynaptic $[Ca^{2+}]_i$ changes in response to mild to moderate depolarization (10–50 mM KCl), we used the high-affinity Ca^{2+} indicator Fura-2, while the low-affinity Ca^{2+} indicator Fura-FF was employed for monitoring $[Ca^{2+}]_i$ produced by the stronger stimuli such as 90 mM KCl and 1 μM capsaicin. Since the excitation spectra of Fura-2 (Fura-FF) and mtPericam overlap significantly, the measurements of $[Ca^{2+}]_i$ and $[Ca^{2+}]_{mt}$ were carried out in parallel experiments. Figure 8 shows representative presynaptic $[Ca^{2+}]_i$ and $[Ca^{2+}]_{mt}$ traces in response to incremental depolarization. $[Ca^{2+}]_i$ changes in axonal boutons were detectable in response to 10 mM KCl, whereas triggering $[Ca^{2+}]_{mt}$ response required 15 mM KCl to produce a stronger depolarization. Analysis of the initial rate of the $[Ca^{2+}]_{mt}$ rise as a function of presynaptic $[Ca^{2+}]_i$ elevations showed that Ca^{2+} uptake by mitochondria was induced by a $[Ca^{2+}]_i$ elevation as little as 200–300 nM ($K_{0.5}$ ~ 600 nM); the rate of $[Ca^{2+}]_{mt}$ rise (V_{MCU}) progressively increased with the $[Ca^{2+}]_i$ increase, until V_{MCU} reached its maximum once $[Ca^{2+}]_i$ began to exceed ~2 μM (Fig. 8*E*). Thus, the mitochondrial Ca^{2+} uptake mechanism in axonal boutons of DRG neurons is highly sensitive to cytosolic Ca^{2+}. Moreover, the Hill coefficient was 2.3, suggesting that MCU activation by Ca^{2+} is cooperative (Fig. 8*E*).

Finally, we examined the expression of several recently identified components of mitochondrial Ca^{2+}

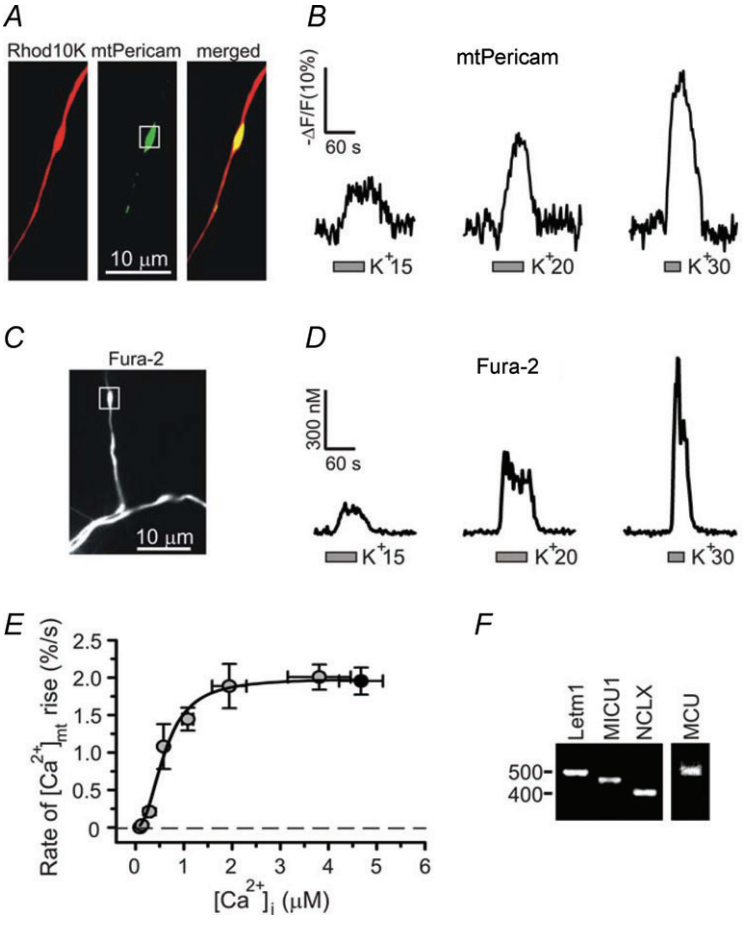

Figure 8. Quantification of mitochondrial Ca^{2+} uptake as a function of $[Ca^{2+}]_i$ elevation
A, DRG neurons were transfected with mtPericam (green) and subsequently loaded with Rhod10K to identify presynaptic boutons. *B*, $[Ca^{2+}]_{mt}$ changes in axonal boutons (white box) were evoked by depolarization of incremental magnitude using solutions containing 15 mM KCl, 20 mM KCl or 30 mM KCl. *C*, axonal distribution of Fura-2 in a resting DRG neuron. *D*, $[Ca^{2+}]_i$ changes in axonal boutons (white box) recorded in Fura-2-loaded DRG neurons using the same stimulation protocol as in *B*. *E*, the initial rate of the $[Ca^{2+}]_{mt}$ increase is plotted as a function of peak $[Ca^{2+}]_i$ elevation in response to K^+-induced depolarization or TRPV1 stimulation. $[Ca^{2+}]_i$ and $[Ca^{2+}]_{mt}$ changes were evoked by applying 10, 15, 20, 30, 50 or 90 mM KCl (30 s, grey; n = 8–24 boutons from 4–8 cells) or 1 μM capsaicin (30 s; black; n = 16 boutons/5 cells for $[Ca^{2+}]_i$ and n = 15 boutons/4 cells for $[Ca^{2+}]_{mt}$), as described in *B* and *D*. $[Ca^{2+}]_i$ was measured using Fura-2 (10, 15, 20, 30 and 50 mM KCl) or Fura-FF (90 mM KCl and 1 μM capsaicin); $[Ca^{2+}]_{mt}$ was measured using mtPericam. The initial rate of rise in $[Ca^{2+}]_{mt}$ was calculated by dividing half of the $[Ca^{2+}]_{mt}$ amplitude by the time required to reach half of the $[Ca^{2+}]_{mt}$ peak. The data were fitted using the Hill equation (Origin 7 software), which produced a $K_{0.5}$ = 606 nM and a Hill coefficient = 2.3. *F*, RT-PCR analysis of neuron-enriched DRG culture shows that several putative molecular components of mitochondrial Ca^{2+} transport, Letm1, MCU, MICU1 and NCLX, are expressed in DRG neurons.

transport. MCU has been proposed to mediate mitochondrial Ca^{2+} uptake (Baughman *et al.* 2011; De Stefani *et al.* 2011), whereas the $Na^+/Ca^{2+}/Li^+$ exchanger (NCLX) is probably responsible for mitochondrial Na^+/Ca^{2+} exchange (Palty *et al.* 2010). Leucine zipper EF hand-containing transmembrane protein (Letm1) was identified as a mitochondrial Ca^{2+}/H^+ antiporter that can contribute to both mitochondrial Ca^{2+} uptake and release, depending on the mitochondrial Ca^{2+} concentration (Jiang *et al.* 2009). In addition, the mitochondrial calcium uptake 1 (MICU1) has been proposed to function as an essential regulator of mitochondrial Ca^{2+} uptake (Perocchi *et al.* 2010; Mallilankaraman *et al.* 2012). RT-PCR analysis of RNA extracted from neuron-enriched DRG cultures demonstrated the presence of all four transcripts (Fig. 8*F*).

Discussion

The present study identifies mechanisms of presynaptic $[Ca^{2+}]_i$ regulation in an *in vitro* model of the first sensory synapse. This synapse controls nociceptive transmission from the periphery to the CNS, and plasticity at this synapse contributes to bidirectional modulation of pain processing (Ji *et al.* 2003; Woolf & Salter, 2006; Kuner, 2010; Ruscheweyh *et al.* 2011). We found that presynaptic $[Ca^{2+}]_i$ in DRG is at ∼100 nM at rest, and that this low baseline $[Ca^{2+}]_i$ is maintained by Ca^{2+} extrusion via PMCA and NCX, as well by Ca^{2+} buffering into intracellular Ca^{2+} organelles. Presynaptic $[Ca^{2+}]_i$ transients induced by brief electrical stimulation rapidly recovered to the baseline with a time constant of ∼2 s. The ER Ca^{2+} pumps did not significantly contribute to presynaptic $[Ca^{2+}]_i$ clearance at this synapse under the described stimulation conditions. On the other hand, PMCA-mediated Ca^{2+} extrusion and Ca^{2+} uptake by presynaptic mitochondria had major impacts on the rate of $[Ca^{2+}]_i$ clearance, accounting for ∼47 and 40%, respectively, of the $[Ca^{2+}]_i$ recovery. Ca^{2+} imaging in presynaptic mitochondria revealed a high sensitivity of MCU to $[Ca^{2+}]_i$ elevations, with 3–5 action potentials being sufficient to produce detectable Ca^{2+} uptake by presynaptic mitochondria. Quantification of the rate of mitochondrial Ca^{2+} uptake as a function of $[Ca^{2+}]_i$ yielded a $K_{0.5}$ of ∼600 nM, and a Hill coefficient of 2.3. These values are consistent with the high Ca^{2+} affinity of presynaptic MCU ($K_{0.5}$ ∼ 0.4–0.5 μM) reported for non-mammalian synapses (David, 1999; Chouhan *et al.* 2010). In addition, the Hill coefficient of 2.3 is similar to the previously reported value of ∼2 for isolated mitochondria and intact cells (Gunter & Pfeiffer, 1990; Colegrove *et al.* 2000), and suggests that Ca^{2+} cooperatively binds to and activates MCU in the presynaptic mitochondria of DRG neurons.

Our finding that presynaptic $[Ca^{2+}]_i$ recovers in DRG neurons with $\tau \sim 2$ s is in good agreement with the $[Ca^{2+}]_i$ recovery rates reported for presynaptic boutons in the hippocampus (1–3 s) (Scotti *et al.* 1999; Scott & Rusakov, 2006) and neurohypophysial axonal terminals (1–2 s) (Lee *et al.* 2002), although faster $[Ca^{2+}]_i$ clearance kinetics have been observed in presynaptic terminals of Purkinje and cerebellar granule cells (τ ∼ 200–300 ms) (Mintz *et al.* 1995; Regehr & Atluri, 1995). Our data are also in good agreement with the observations in human nociceptive C-fibres, where electrically evoked $[Ca^{2+}]_i$ transients recovered to baseline with a half-recovery time of ∼2–3 s (Mayer *et al.* 1999). However, a 5–10-fold slower rate of $[Ca^{2+}]_i$ clearance was reported for sensory terminals of the rat cornea (Gover *et al.* 2007*b*), suggesting that Ca^{2+} clearance mechanisms at these sensory terminals originating from the trigeminal ganglia appear to be quite different from those in the peripheral and central processes of DRG neurons. This may not be surprising given that mitochondria do not participate in $[Ca^{2+}]_i$ clearance from corneal terminals (Gover *et al.* 2007*b*), but significantly impact presynaptic $[Ca^{2+}]_i$ recovery in DRG neurons (Figs 5 and 6). It is also possible that use of the high-affinity Ca^{2+} indicator Oregon Green BAPTA-1 dextran (K_d∼170 nM) to measure $[Ca^{2+}]_i$ in the corneal terminals (Gover *et al.* 2007*b*) might have also contributed to a slowed rate of $[Ca^{2+}]_i$ recovery in that work (Neher & Augustine, 1992; Kirischuk *et al.* 1999).

Our finding that SERCA does not significantly contribute to presynaptic Ca^{2+} clearance in DRG neurons (Fig. 4) is somewhat surprising given that SERCA plays major roles in setting the duration and amplitude of $[Ca^{2+}]_i$ responses in the somata of DRG and trigeminal sensory neurons (Usachev & Thayer, 1999; Lu *et al.* 2006; Gover *et al.* 2007*a*; Rigaud *et al.* 2009). Just the same, our data are consistent with a negligible role of SERCA in peripheral sensory terminals of the cornea (Gover *et al.* 2007*b*), suggesting that the impact of SERCA on $[Ca^{2+}]_i$ regulation differs substantially between the cell body and axons in sensory neurons. However, we cannot rule out the possibility that SERCA blockade led to enhanced function of PMCA or other Ca^{2+} transporters, thereby masking the effects of SERCA inhibitors. It is likely that the presynaptic boutons of primary sensory neurons contain functional intracellular Ca^{2+} stores associated with the ER. First, the SERCA inhibitor Tg was shown to modulate glutamate release at the first sensory synapse (Tsuzuki *et al.* 2004). Second, we found that an activator of ryanodine receptors, caffeine, induced Ca^{2+} release from the intracellular stores in presynaptic boutons of DRG neurons (Fig. 4*D*). Although SERCA pumps do not contribute significantly to the rate of presynaptic $[Ca^{2+}]_i$ recovery, Ca^{2+} stores are involved in the maintenance of low $[Ca^{2+}]_i$ at rest, as the SERCA inhibitors CPA and Tg produced 20–50 nM elevation of the $[Ca^{2+}]_i$ baseline.

The latter could be explained either by activation of Ca^{2+} influx through presynaptic store-operated Ca^{2+} channels (Usachev & Thayer, 1999; Gemes *et al.* 2011) or the role of SERCA pumps in controlling presynaptic $[Ca^{2+}]_i$ at rest.

Na^+/Ca^{2+} exchange of the plasma membrane is another mechanism that can contribute to Ca^{2+} clearance. Based on our RT-PCR data (Fig. 2*D*), DRG neurons express three Na^+/Ca^{2+} exchanger isoforms that are K^+-independent (NCX1, NCX2 and NCX3) and one that is K^+-dependent (NCKX2). The functional analysis showed that plasma membrane Na^+/Ca^{2+} exchange regulated the resting $[Ca^{2+}]_i$ and contributed approximately 12% to presynaptic Ca^{2+} clearance in DRG neurons (Fig. 2), and that this transport was probably mediated by the NCX, but not NCKX, isoforms (Fig. 2*E*). Only limited information is available about the specific roles of NCX and NCKX at various synapses. NCKX was shown to be the major mechanism mediating Ca^{2+} extrusion from axonal terminals of the rat neurohypophysis (Lee *et al.* 2002), whereas both NCX and NCKX contribute to presynaptic $[Ca^{2+}]_i$ clearance at the calyx of Held synapse (Kim *et al.* 2005). Notably, deletion of NCX2 results in increased paired-pulsed facilitation of synaptic transmission and enhanced LTP in the CA1 region of the hippocampus (Jeon *et al.* 2003), whereas deletion of NCKX2 leads to a profound loss of the hippocampal LTP (Li *et al.* 2006). Thus, it is likely that the NCX and NCKX isoforms play distinct roles at various synapses.

Identification of PMCA as a key regulator of presynaptic $[Ca^{2+}]_i$ at the sensory synapses is in agreement with the major role of PMCA in controlling $[Ca^{2+}]_i$ recovery in the somata of DRG and trigeminal sensory neurons (Benham *et al.* 1992; Usachev *et al.* 2002; Gover *et al.* 2007*a*), as well as in peripheral sensory terminals innervating the cornea (Gover *et al.* 2007*b*). PMCA is a high-affinity (0.1–0.2 μM) ATP-dependent Ca^{2+} transporter that extrudes Ca^{2+} from the cell (Carafoli, 1991; Elwess *et al.* 1997). The PMCA family of proteins consist of four major isoforms, PMCA1–4, and alternative RNA splicing of these gives rise to nearly 30 PMCA proteins that differ in their tissue distribution, function and regulatory properties (Strehler & Zacharias, 2001; Thayer *et al.* 2002). PMCA2 (splice variants 2a and 2b) and PMCA4 (splice variant 4b) are the major PMCA isoforms expressed in the DRG (Usachev *et al.* 2002). PMCA4 is highly expressed in the superficial lamina of the dorsal horn, where the majority of TRPV1-positive sensory fibres terminate; PMCA2, on the other hand, is found in the deeper lamina of the dorsal horn (Tachibana *et al.* 2004). PMCA2 has very high affinity for Ca^{2+} ($\sim$0.09 μM for PMCA2a and $\sim$0.06 μM for PMCA2b), suggesting that it plays an important role in maintaining low resting $[Ca^{2+}]_i$ (Elwess *et al.* 1997). PMCA4b exhibits a somewhat lower apparent affinity for Ca^{2+} ($\sim$0.16 μM) (Elwess *et al.* 1997), but its activity can be markedly increased by PKC-mediated phosphorylation (Enyedi *et al.* 1996). Notably, this mechanism is responsible for a marked PKC-mediated acceleration of Ca^{2+} efflux from the somata and axonal boutons of DRG neurons (Usachev *et al.* 2002).

PMCA2 and PMCA4 are also highly sensitive to stimulation by calmodulin (CaM). Ca^{2+}-dependent binding of CaM to the PMCA autoinhibitory domain, located in its carboxy-terminus, disinhibits the pump, which results in a marked increase of both Ca^{2+} affinity and maximal velocity (V_{max}) of PMCA (Carafoli, 1991; Strehler & Zacharias, 2001). The two major PMCA isoforms in DRG neurons, PMCA2b and PMCA4b (Usachev *et al.* 2002), are characterized by unusually slow dissociation of CaM (>20 min) (Caride *et al.* 1999, 2001). This implies that even a brief elevation in $[Ca^{2+}]_i$ will produce a long-lasting CaM/Ca^{2+}-dependent stimulation of PMCA. Indeed, a priming $[Ca^{2+}]_i$ elevation has been reported to result in long-term enhancement of Ca^{2+} extrusion ($\sim$1 h) in DRG neurons (Pottorf & Thayer, 2002). Thus, PMCA-mediated Ca^{2+} extrusion in sensory neurons is subject to modulation by both neuronal activity and PKC. In the context of spinal pain processing, the described mechanisms are predicted to accelerate presynaptic $[Ca^{2+}]_i$ clearance during central sensitization, which is known to be associated with heightened neuronal activity in the spinal cord and enhanced release of neuromodulators coupled to PKC signalling (e.g. bradykinin and substance P). However, direct testing of this idea is hampered by a lack of isoform-specific inhibitors of PMCA and technical difficulties associated with presynaptic Ca^{2+} imaging in spinal cord slices or *in vivo*.

Ca^{2+} uptake by presynaptic mitochondria is another major mechanism responsible for presynaptic $[Ca^{2+}]_i$ clearance in DRG neurons. Electron microscopy has demonstrated numerous presynaptic mitochondria in the central processes of primary sensory neurons, including TRPV1-expressing boutons (Maxwell & Rethelyi, 1987; Rethelyi *et al.* 1989; Hwang *et al.* 2003). We also found that axonal boutons are intensely labelled by the mitochondria-targeted Ca^{2+} indicator mtPericam (Medvedeva *et al.* 2008; Figs 7 and 8). Presynaptic clustering of mitochondria is consistent with the high energy demand at the synapses. Mitochondria also play important roles in shaping presynaptic $[Ca^{2+}]_i$ signals at various synapses (Billups & Forsythe, 2002; David & Barrett, 2003; Jonas, 2004; Garcia-Chacon *et al.* 2006; Lee *et al.* 2007*a*), including the first sensory synapse (Medvedeva *et al.* 2008; Figs 5 and 6). Mitochondria buffer excessive Ca^{2+} via the Ca^{2+} uniporter mechanism, and subsequently release accumulated Ca^{2+} back into the cytosol via Na^+/Ca^{2+} exchange or other mechanisms (Bernardi, 1999). Ca^{2+} buffering by mitochondria limits the amplitude of the cytosolic $[Ca^{2+}]_i$ elevation, and

accelerates the initial recovery of presynaptic $[Ca^{2+}]_i$ (Medvedeva *et al.* 2008; Figs 5 and 6). Our data suggest that the impact of mitochondria on the amplitude of presynaptic $[Ca^{2+}]_i$ responses is much greater than that of PMCA (FCCP or RuR induced ∼60–100% increase in the amplitude of $[Ca^{2+}]_i$ response compared to ∼20% increase produced by pH 8.8). One possible explanation of this difference is that Ca^{2+} transport by the mitochondrial uniporter is much faster than that by PMCA (Miller, 1991; Elwess *et al.* 1997; Gunter & Sheu, 2009).

Our comparison of the time courses of $[Ca^{2+}]_i$ and $[Ca^{2+}]_{mt}$ changes induced by electrical stimulation demonstrated that $[Ca^{2+}]_{mt}$ reaches its peak by 1–2 s later than presynaptic $[Ca^{2+}]_i$ (Fig. 7*D*), indicating that mitochondrial Ca^{2+} uptake continues during the initial phase of $[Ca^{2+}]_i$ recovery. This observation is consistent with the role of mitochondrial Ca^{2+} uptake in $[Ca^{2+}]_i$ recovery in the axonal boutons of DRG neurons. Based on the effects of the mitochondrial Ca^{2+} uniporter inhibitor RuR, we estimate that mitochondria account for at least 40% of the $[Ca^{2+}]_i$ recovery in the axonal boutons of DRG neurons. Although our analysis using the protonophore FCCP suggested that MCU has a somewhat stronger effect on the rate of presynaptic Ca^{2+} clearance (∼54%), this difference could be due to a partial inhibition of ATP synthesis by FCCP.

Ca^{2+} initially accumulated by mitochondria can be subsequently released back into the cytosol. Following intense (e.g. tetanic) stimulation, strong Ca^{2+} efflux from mitochondria can markedly slow recovery of presynaptic $[Ca^{2+}]_i$ leading to a $[Ca^{2+}]_i$ plateau lasting many minutes after stimulation is terminated (Tang & Zucker, 1997; Garcia-Chacon *et al.* 2006; Lee *et al.* 2007*a*). We previously reported that TRPV1 activation or intense electrical stimulation (20 Hz for 30 s) results in a long-lasting presynaptic $[Ca^{2+}]_i$ plateau associated with enhanced glutamate release in DRG neurons (Medvedeva *et al.* 2008). In contrast, mild electrical stimulation such as that used in the present study (10 Hz for 2 s) was insufficient to generate a $[Ca^{2+}]_i$ plateau in the same axonal boutons, in spite of the contribution of mitochondria to Ca^{2+} clearance. Thus, a specific role of presynaptic mitochondria at the sensory synapse depends on the type and intensity of the stimulus.

In addition to regulating presynaptic $[Ca^{2+}]_i$, mitochondrial Ca^{2+} uptake can stimulate the production of ATP via Ca^{2+}-dependent dehydrogenases (Hajnoczky *et al.* 1995; Denton, 2009; Chouhan *et al.* 2012) and the generation of reactive oxygen species (ROS) (Nicholls & Budd, 2000; Hongpaisan *et al.* 2004). Both effects require strong neuronal activation (Hongpaisan *et al.* 2004; Chouhan *et al.* 2012), and this probably explains why mitochondrial Ca^{2+} uptake following the mild stimulation used in our study did not detectably impact ATP-dependent Ca^{2+} transport (Fig. 6*D*–*F*). In pathological pain states, neuronal activity in the spinal cord is markedly intensified, and the resulting enhancement of ROS production is thought to contribute to central sensitization (Schwartz *et al.* 2009). Notably, recent data suggest that mitochondrial Ca^{2+} uptake is essential for ROS-dependent plasticity in the spinal cord, and for the development of persistent pain (Kim *et al.* 2011).

In summary, this study provides the first detailed characterization of Ca^{2+} clearance mechanisms in presynaptic boutons of DRG neurons, and identifies PMCA and mitochondria as major regulators of Ca^{2+} signalling at the first sensory synapse. Development of new pharmacological and genetic tools targeting specific PMCA isoforms and mitochondrial Ca^{2+} transporters will be required to determine their precise contribution to the various forms of synaptic plasticity involved in spinal pain processing, such as wind-up, LTP and central sensitization.

References

Annunziato L, Pignataro G & Di Renzo GF (2004). Pharmacology of brain Na^+/Ca^{2+} exchanger: from molecular biology to therapeutic perspectives. *Pharmacol Rev* **56**, 633–654.

Bao J, Li JJ & Perl ER (1998). Differences in Ca^{2+} channels governing generation of miniature and evoked excitatory synaptic currents in spinal laminae I and II. *J Neurosci* **18**, 8740–8750.

Baughman JM, Perocchi F, Girgis HS, Plovanich M, Belcher-Timme CA, Sancak Y, Bao XR, Strittmatter L, Goldberger O, Bogorad RL, Koteliansky V & Mootha VK (2011). Integrative genomics identifies MCU as an essential component of the mitochondrial calcium uniporter. *Nature* **476**, 341–345.

Benham CD, Evans ML & McBain CJ (1992). Ca^{2+} efflux mechanisms following depolarization evoked calcium transients in cultured rat sensory neurones. *J Physiol* **455**, 567–583.

Bernardi P (1999). Mitochondrial transport of cations: channels, exchangers, and permeability transition. *Physiol Rev* **79**, 1127–1155.

Billups B & Forsythe ID (2002). Presynaptic mitochondrial calcium sequestration influences transmission at mammalian central synapses. *J Neurosci* **22**, 5840–5847.

Blaustein MP & Lederer WJ (1999). Sodium/calcium exchange: its physiological implications. *Physiol Rev* **79**, 763–854.

Cao YQ (2006). Voltage-gated calcium channels and pain. *Pain* **126**, 5–9.

Carafoli E (1991). Calcium pump of the plasma membrane. *Physiol Rev* **71**, 129–153.

Caride AJ, Elwess NL, Verma AK, Filoteo AG, Enyedi A, Bajzer Z & Penniston JT (1999). The rate of activation by calmodulin of isoform 4 of the plasma membrane Ca^{2+} pump is slow and is changed by alternative splicing. *J Biol Chem* **274**, 35227–35232.

Caride AJ, Penheiter AR, Filoteo AG, Bajzer Z, Enyedi A & Penniston JT (2001). The plasma membrane calcium pump displays memory of past calcium spikes. Differences between isoforms 2b and 4b. *J Biol Chem* **276**, 39797–39804.

Caterina MJ & Julius D (2001). The vanilloid receptor: a molecular gateway to the pain pathway. *Annu Rev Neurosci* **24**, 487–517.

Cavanaugh DJ, Chesler AT, Jackson AC, Sigal YM, Yamanaka H, Grant R, O'Donnell D, Nicoll RA, Shah NM, Julius D & Basbaum AI (2011). Trpv1 reporter mice reveal highly restricted brain distribution and functional expression in arteriolar smooth muscle cells. *J Neurosci* **31**, 5067–5077.

Chouhan AK, Ivannikov MV, Lu Z, Sugimori M, Llinas RR & Macleod GT (2012). Cytosolic calcium coordinates mitochondrial energy metabolism with presynaptic activity. *J Neurosci* **32**, 1233–1243.

Chouhan AK, Zhang J, Zinsmaier KE & Macleod GT (2010). Presynaptic mitochondria in functionally different motor neurons exhibit similar affinities for Ca^{2+} but exert little influence as Ca^{2+} buffers at nerve firing rates *in situ*. *J Neurosci* **30**, 1869–1881.

Clayton EL & Cousin MA (2009). The molecular physiology of activity-dependent bulk endocytosis of synaptic vesicles. *J Neurochem* **111**, 901–914.

Colegrove SL, Albrecht MA & Friel DD (2000). Quantitative analysis of mitochondrial Ca^{2+} uptake and release pathways in sympathetic neurons – Reconstruction of the recovery after depolarization-evoked $[Ca^{2+}]_i$ elevations. *J Gen Physiol* **115**, 371–388.

Cousin MA & Robinson PJ (2001). The dephosphins: dephosphorylation by calcineurin triggers synaptic vesicle endocytosis. *Trends Neurosci* **24**, 659–665.

David G (1999). Mitochondrial clearance of cytosolic Ca^{2+} in stimulated lizard motor nerve terminals proceeds without progressive elevation of mitochondrial matrix $[Ca^{2+}]$. *J Neurosci* **19**, 7495–7506.

David G & Barrett EF (2003). Mitochondrial Ca^{2+} uptake prevents desynchronization of quantal release and minimizes depletion during repetitive stimulation of mouse motor nerve terminals. *J Physiol* **548**, 425–438.

De Stefani D, Raffaello A, Teardo E, Szabo I & Rizzuto R (2011). A forty-kilodalton protein of the inner membrane is the mitochondrial calcium uniporter. *Nature* **476**, 336–340.

Denton RM (2009). Regulation of mitochondrial dehydrogenases by calcium ions. *Biochim Biophys Acta* **1787**, 1309–1316.

Elwess NL, Filoteo AG, Enyedi A & Penniston JT (1997). Plasma membrane Ca^{2+} pump isoforms 2a and 2b are unusually responsive to calmodulin and Ca^{2+}. *J Biol Chem* **272**, 17981–17986.

Empson RM, Garside ML & Knopfel T (2007). Plasma membrane Ca^{2+} ATPase 2 contributes to short-term synapse plasticity at the parallel fiber to Purkinje neuron synapse. *J Neurosci* **27**, 3753–3758.

Enyedi A, Verma AK, Filoteo AG & Penniston JT (1996). Protein kinase C activates the plasma membrane Ca^{2+} pump isoform 4b by phosphorylation of an inhibitory region downstream of the calmodulin-binding domain. *J Biol Chem* **271**, 32461–32467.

Garcia-Chacon LE, Nguyen KT, David G & Barrett EF (2006). Extrusion of Ca^{2+} from mouse motor terminal mitochondria via a Na^+-Ca^{2+} exchanger increases post-tetanic evoked release. *J Physiol* **574**, 663–675.

Gemes G, Bangaru ML, Wu HE, Tang Q, Weihrauch D, Koopmeiners AS, Cruikshank JM, Kwok WM & Hogan QH (2011). Store-operated Ca^{2+} entry in sensory neurons: functional role and the effect of painful nerve injury. *J Neurosci* **31**, 3536–3549.

Gover TD, Moreira TH, Kao JP & Weinreich D (2007*a*). Calcium homeostasis in trigeminal ganglion cell bodies. *Cell Calcium* **41**, 389–396.

Gover TD, Moreira TH, Kao JP & Weinreich D (2007*b*). Calcium regulation in individual peripheral sensory nerve terminals of the rat. *J Physiol* **578**, 481–490.

Groffen AJ, Martens S, Diez Arazola R, Cornelisse LN, Lozovaya N, de Jong AP, Goriounova NA, Habets RL, Takai Y, Borst JG, Brose N, McMahon HT & Verhage M (2010). Doc2b is a high-affinity Ca^{2+} sensor for spontaneous neurotransmitter release. *Science* **327**, 1614–1618.

Gruner W & Silva LR (1994). ω-Conotoxin sensitivity and presynaptic inhibition of glutamatergic sensory neurotransmission *in vitro*. *J Neurosci* **14**, 2800–2808.

Grynkiewicz G, Poenie M & Tsien RY (1985). A new generation of Ca^{2+} indicators with greatly improved fluorescence properties. *J Biol Chem* **260**, 3440–3450.

Gu JGG & Macdermott AB (1997). Activation of ATP P2x receptors elicits glutamate release from sensory neuron synapses. *Nature* **389**, 749–753.

Gunter TE & Pfeiffer DR (1990). Mechanisms by which mitochondria transport calcium. *Am J Physiol* **258**, C755–C786.

Gunter TE & Sheu SS (2009). Characteristics and possible functions of mitochondrial Ca^{2+} transport mechanisms. *Biochim Biophys Acta* **1787**, 1291–1308.

Guo A, Vulchanova L, Wang J, Li X & Elde R (1999). Immunocytochemical localization of the vanilloid receptor 1 (VR1): relationship to neuropeptides, the P2′3 purinoceptor and IB4 binding sites. *Eur J Neurosci* **11**, 946–958.

Hajnoczky G, Robb GL, Seitz MB & Thomas AP (1995). Decoding of cytosolic calcium oscillations in the mitochondria. *Cell* **82**, 415–424.

Heinke B, Balzer E & Sandkuhler J (2004). Pre- and postsynaptic contributions of voltage-dependent Ca^{2+} channels to nociceptive transmission in rat spinal lamina I neurons. *Eur J Neurosci* **19**, 103–111.

Heinke B, Gingl E & Sandkuhler J (2011). Multiple targets of μ-opioid receptor-mediated presynaptic inhibition at primary afferent Aδ- and C-fibers. *J Neurosci* **31**, 1313–1322.

Henzi V & MacDermott AB (1992). Characteristics and function of Ca^{2+}- and inositol 1,4,5-trisphosphate-releasable stores of Ca^{2+} in neurons. *Neuroscience* **46**, 251–273.

Hernandez-Guijo JM, Maneu-Flores VE, Ruiz-Nuno A, Villarroya M, Garcia AG & Gandia L (2001). Calcium-dependent inhibition of L, N, and P/Q Ca^{2+} channels in chromaffin cells: role of mitochondria. *J Neurosci* **21**, 2553–2560.

Hollenbeck PJ (2005). Mitochondria and neurotransmission: evacuating the synapse. *Neuron* **47**, 331–333.

Hongpaisan J, Winters CA & Andrews SB (2004). Strong calcium entry activates mitochondrial superoxide generation, upregulating kinase signaling in hippocampal neurons. *J Neurosci* **24**, 10878–10887.

Huang SM, Bisogno T, Trevisani M, Al-Hayani A, De Petrocellis L, Fezza F, Tognetto M, Petros TJ, Krey JF, Chu CJ, Miller JD, Davies SN, Geppetti P, Walker JM & Di Marzo V (2002). An endogenous capsaicin-like substance with high potency at recombinant and native vanilloid VR1 receptors. *Proc Natl Acad Sci U S A* **99**, 8400–8405.

Hwang SJ, Burette A & Valtschanoff JG (2003). VR1-positive primary afferents contact NK1-positive spinoparabrachial neurons. *J Comp Neurol* **460**, 255–265.

Jeon D, Yang YM, Jeong MJ, Philipson KD, Rhim H & Shin HS (2003). Enhanced learning and memory in mice lacking Na^+/Ca^{2+} exchanger 2. *Neuron* **38**, 965–976.

Ji RR, Kohno T, Moore KA & Woolf CJ (2003). Central sensitization and LTP: do pain and memory share similar mechanisms? *Trends Neurosci* **26**, 696–705.

Jiang D, Zhao L & Clapham DE (2009). Genome-wide RNAi screen identifies Letm1 as a mitochondrial Ca^{2+}/H^+ antiporter. *Science* **326**, 144–147.

Jonas E (2004). Regulation of synaptic transmission by mitochondrial ion channels. *J Bioenerg Biomembr* **36**, 357–361.

Junge HJ, Rhee JS, Jahn O, Varoqueaux F, Spiess J, Waxham MN, Rosenmund C & Brose N (2004). Calmodulin and Munc13 form a Ca^{2+} sensor/effector complex that controls short-term synaptic plasticity. *Cell* **118**, 389–401.

Kim HY, Lee KY, Lu Y, Wang J, Cui L, Kim SJ, Chung JM & Chung K (2011). Mitochondrial Ca^{2+} uptake is essential for synaptic plasticity in pain. *J Neurosci* **31**, 12982–12991.

Kim MH, Korogod N, Schneggenburger R, Ho WK & Lee SH (2005). Interplay between Na^+/Ca^{2+} exchangers and mitochondria in Ca^{2+} clearance at the calyx of Held. *J Neurosci* **25**, 6057–6065.

Kirischuk S, Veselovsky N & Grantyn R (1999). Single-bouton-mediated synaptic transmission: postsynaptic conductance changes in their relationship with presynaptic calcium signals. *Pflugers Arch* **438**, 716–724.

Kuner R (2010). Central mechanisms of pathological pain. *Nat Med* **16**, 1258–1266.

Lee D, Lee KH, Ho WK & Lee SH (2007*a*). Target cell-specific involvement of presynaptic mitochondria in post-tetanic potentiation at hippocampal mossy fiber synapses. *J Neurosci* **27**, 13603–13613.

Lee JY, Ho WK & Lee SH (2007*b*). Ionic selectivity of NCKX2, NCKX3, and NCKX4 for monovalent cations at K^+-binding site. *Ann N Y Acad Sci* **1099**, 166–170.

Lee SH, Kim MH, Park KH, Earm YE & Ho WK (2002). K^+-dependent Na^+/Ca^{2+} exchange is a major Ca^{2+} clearance mechanism in axon terminals of rat neurohypophysis. *J Neurosci* **22**, 6891–6899.

Li XF, Kiedrowski L, Tremblay F, Fernandez FR, Perizzolo M, Winkfein RJ, Turner RW, Bains JS, Rancourt DE & Lytton J (2006). Importance of K^+-dependent Na^+/Ca^{2+}-exchanger 2, NCKX2, in motor learning and memory. *J Biol Chem* **281**, 6273–6282.

Lu SG, Zhang X & Gold MS (2006). Intracellular calcium regulation among subpopulations of rat dorsal root ganglion neurons. *J Physiol* **577**, 169–190.

Ly CV & Verstreken P (2006). Mitochondria at the synapse. *Neuroscientist* **12**, 291–299.

Lytton J (2007). Na^+/Ca^{2+} exchangers: three mammalian gene families control Ca^{2+} transport. *Biochem J* **406**, 365–382.

Mallilankaraman K, Doonan P, Cardenas C, Chandramoorthy HC, Muller M, Miller R, Hoffman NE, Gandhirajan RK, Molgo J, Birnbaum MJ, Rothberg BS, Mak DO, Foskett JK & Madesh M (2012). MICU1 is an essential gatekeeper for MCU-mediated mitochondrial Ca^{2+} uptake that regulates cell survival. *Cell* **151**, 630–644.

Mata AM & Sepulveda MR (2005). Calcium pumps in the central nervous system. *Brain Res Brain Res Rev* **49**, 398–405.

Maxwell D & Rethelyi M (1987). Ultrastructure and synaptic connections of cutaneous afferent fibers in the spinal cord. *Trends Neurosci* **10**, 117–123.

Mayer C, Quasthoff S & Grafe P (1999). Confocal imaging reveals activity-dependent intracellular Ca^{2+} transients in nociceptive human C fibres. *Pain* **81**, 317–322.

McGivern JG (2006). Targeting N-type and T-type calcium channels for the treatment of pain. *Drug Discov Today* **11**, 245–253.

Medvedeva YV, Kim MS, Schnizler K & Usachev YM (2009). Functional tetrodotoxin-resistant Na^+ channels are expressed presynaptically in rat dorsal root ganglia neurons. *Neuroscience* **159**, 559–569.

Medvedeva YV, Kim MS & Usachev YM (2008). Mechanisms of prolonged presynaptic Ca^{2+} signaling and glutamate release induced by TRPV1 activation in rat sensory neurons. *J Neurosci* **28**, 5295–5311.

Meyer RA & Campbell JN (1981). Myelinated nociceptive afferents account for the hyperalgesia that follows a burn to the hand. *Science* **213**, 1527–1529.

Miller RJ (1991). The control of neuronal Ca^{2+} homeostasis. *Prog Neurobiol* **37**, 255–285.

Mintz IM, Sabatini BL & Regehr WG (1995). Calcium control of transmitter release at a cerebellar synapse. *Neuron* **15**, 675–688.

Nagai T, Sawano A, Park ES & Miyawaki A (2001). Circularly permuted green fluorescent proteins engineered to sense Ca^{2+}. *Proc Natl Acad Sci U S A* **98**, 3197–3202.

Neher E & Augustine GJ (1992). Calcium gradients and buffers in bovine chromaffin cells. *J Physiol* **450**, 273–301.

Neher E & Sakaba T (2008). Multiple roles of calcium ions in the regulation of neurotransmitter release. *Neuron* **59**, 861–872.

Nicholls DG & Budd SL (2000). Mitochondria and neuronal survival. *Physiol Rev* **80**, 315–360.

Nicholls DG & Ward MW (2000). Mitochondrial membrane potential and neuronal glutamate excitotoxicity: mortality and millivolts. *Trends Neurosci* **23**, 166–174.

Palty R, Silverman WF, Hershfinkel M, Caporale T, Sensi SL, Parnis J, Nolte C, Fishman D, Shoshan-Barmatz V, Herrmann S, Khananshvili D & Sekler I (2010). NCLX is an essential component of mitochondrial Na^+/Ca^{2+} exchange. *Proc Natl Acad Sci U S A* **107**, 436–441.

Perocchi F, Gohil VM, Girgis HS, Bao XR, McCombs JE, Palmer AE & Mootha VK (2010). MICU1 encodes a mitochondrial EF hand protein required for Ca^{2+} uptake. *Nature* **467**, 291–296.

Persson AK, Black JA, Gasser A, Cheng X, Fischer TZ & Waxman SG (2010). Sodium-calcium exchanger and multiple sodium channel isoforms in intra-epidermal nerve terminals. *Mol Pain* **6**, 84.

Pottorf WJ & Thayer SA (2002). Transient rise in intracellular calcium produces a long-lasting increase in plasma membrane calcium pump activity in rat sensory neurons. *J Neurochem* **83**, 1002–1008.

Pozzan T, Rizzuto R, Volpe P & Meldolesi J (1994). Molecular and cellular physiology of intracellular calcium stores. *Physiol Rev* **74**, 595–636.

Regehr WG & Atluri PP (1995). Calcium transients in cerebellar granule cell presynaptic terminals. *Biophys J* **68**, 2156–2170.

Rethelyi M, Light AR & Perl ER (1989). Synaptic ultrastructure of functionally and morphologically characterized neurons of the superficial spinal dorsal horn of cat. *J Neurosci* **9**, 1846–1863.

Rigaud M, Gemes G, Weyker PD, Cruikshank JM, Kawano T, Wu HE & Hogan QH (2009). Axotomy depletes intracellular calcium stores in primary sensory neurons. *Anesthesiology* **111**, 381–392.

Ruscheweyh R, Wilder-Smith O, Drdla R, Liu XG & Sandkuhler J (2011). Long-term potentiation in spinal nociceptive pathways as a novel target for pain therapy. *Mol Pain* **7**, 20.

Schwartz ES, Kim HY, Wang J, Lee I, Klann E, Chung JM & Chung K (2009). Persistent pain is dependent on spinal mitochondrial antioxidant levels. *J Neurosci* **29**, 159–168.

Schwiening CJ, Kennedy HJ & Thomas RC (1993). Calcium hydrogen exchange by the plasma membrane Ca-ATPase of voltage-clamped snail neurons. *Proc R Soc Lond* **253**, 285–289.

Scott R & Rusakov DA (2006). Main determinants of presynaptic Ca^{2+} dynamics at individual mossy fiber-CA3 pyramidal cell synapses. *J Neurosci* **26**, 7071–7081.

Scotti AL, Chatton JY & Reuter H (1999). Roles of Na^{+}-Ca^{2+} exchange and of mitochondria in the regulation of presynaptic Ca^{2+} and spontaneous glutamate release. *Philos Trans R Soc Lond B Biol Sci* **354**, 357–364.

Shmigol A, Kostyuk P & Verkhratsky A (1994). Role of caffeine-sensitive Ca^{2+} stores in Ca^{2+} signal termination in adult mouse DRG neurones. *Neuroreport* **5**, 2073–2076.

Sikand P & Premkumar LS (2007). Potentiation of glutamatergic synaptic transmission by protein kinase C-mediated sensitization of TRPV1 at the first sensory synapse. *J Physiol* **581**, 631–647.

Slugg RM, Meyer RA & Campbell JN (2000). Response of cutaneous A- and C-fiber nociceptors in the monkey to controlled-force stimuli. *J Neurophysiol* **83**, 2179–2191.

Sørensen JB (2004). Formation, stabilisation and fusion of the readily releasable pool of secretory vesicles. *Pflugers Arch* **448**, 347–362.

Spat A, Szanda G, Csordas G & Hajnoczky G (2008). High- and low-calcium-dependent mechanisms of mitochondrial calcium signalling. *Cell Calcium* **44**, 51–63.

Strehler EE & Zacharias DA (2001). Role of alternative splicing in generating isoform diversity among plasma membrane calcium pumps. *Physiol Rev* **81**, 21–50.

Sugita S, Shin OH, Han W, Lao Y & Sudhof TC (2002). Synaptotagmins form a hierarchy of exocytotic Ca^{2+} sensors with distinct Ca^{2+} affinities. *EMBO J* **21**, 270–280.

Szallasi A, Cortright DN, Blum CA & Eid SR (2007). The vanilloid receptor TRPV1: 10 years from channel cloning to antagonist proof-of-concept. *Nat Rev Drug Discov* **6**, 357–372.

Tachibana T, Ogura H, Tokunaga A, Dai Y, Yamanaka H, Seino D & Noguchi K (2004). Plasma membrane calcium ATPase expression in the rat spinal cord. *Brain Res Mol Brain Res* **131**, 26–32.

Tang YG & Zucker RS (1997). Mitochondrial involvement in post-tetanic potentiation of synaptic transmission. *Neuron* **18**, 483–491.

Thayer SA, Usachev YM & Pottorf WJ (2002). Modulating Ca^{2+} clearance from neurons. *Front Biosci* **7**, D1255–1279.

Thomas D & Hanley MR (1994). Pharmacological tools for perturbing intracellular calcium storage. *Methods Cell Biol* **40**, 65–89.

Toescu EC & Verkhratsky A (2003). Neuronal ageing from an intraneuronal perspective: roles of endoplasmic reticulum and mitochondria. *Cell Calcium* **34**, 311–323.

Tsuzuki K, Xing H, Ling J & Gu JG (2004). Menthol-induced Ca^{2+} release from presynaptic Ca^{2+} stores potentiates sensory synaptic transmission. *J Neurosci* **24**, 762–771.

Turner KM, Burgoyne RD & Morgan A (1999). Protein phosphorylation and the regulation of synaptic membrane traffic. *Trends Neurosci* **22**, 459–464.

Usachev YM, DeMarco SJ, Campbell C, Strehler EE & Thayer SA (2002). Bradykinin and ATP accelerate Ca^{2+} efflux from rat sensory neurons via protein kinase C and the plasma membrane Ca^{2+} pump isoform 4. *Neuron* **33**, 113–122.

Usachev YM & Thayer SA (1999). Ca^{2+} influx in resting rat sensory neurones that regulates and is regulated by ryanodine-sensitive Ca^{2+} stores. *J Physiol* **519**, 115–130.

Vangheluwe P, Sepulveda MR, Missiaen L, Raeymaekers L, Wuytack F & Vanoevelen J (2009). Intracellular Ca^{2+}- and Mn^{2+}-transport ATPases. *Chem Rev* **109**, 4733–4759.

Vikman KS, Kristensson K & Hill RH (2001). Sensitization of dorsal horn neurons in a two-compartment cell culture model: wind-up and long-term potentiation-like responses. *J Neurosci* **21**, RC169.

Wanaverbecq N, Marsh SJ, Al-Qatari M & Brown DA (2003). The plasma membrane calcium-ATPase as a major mechanism for intracellular calcium regulation in neurones from the rat superior cervical ganglion. *J Physiol* **550**, 83–101.

Woolf CJ & Salter MW (2006). Plasticity and pain: role of the dorsal horn. In *Textbook of Pain*, ed. McMahon SB & Koltzenburg M, pp. 91–105. Elsevier, Amsterdam.

Xu J, Mashimo T & Sudhof TC (2007). Synaptotagmin-1, -2, and -9: Ca^{2+} sensors for fast release that specify distinct presynaptic properties in subsets of neurons. *Neuron* **54**, 567–581.

Yang K, Kumamoto E, Furue H & Yoshimura M (1998). Capsaicin facilitates excitatory but not inhibitory synaptic transmission in substantia gelatinosa of the rat spinal cord. *Neurosci Lett* **255**, 135–138.

Yao J, Gaffaney JD, Kwon SE & Chapman ER (2011). Doc2 is a Ca^{2+} sensor required for asynchronous neurotransmitter release. *Cell* **147**, 666–677.

Zucker RS & Regehr WG (2002). Short-term synaptic plasticity. *Annu Rev Physiol* **64**, 355–405.

Author contributions

Y.M.U. and L.P.S. designed the work. L.P.S., Y.M.U., M.S.K., P.R.H. and Y.V.M. performed the experiments. Y.M.U. wrote the paper. All authors provided critical intellectual input to the text and figures and approved the final version of the article.

Acknowledgements

This work was supported by National Institutes of Health grant NS072432 and the Fraternal Order of Eagles Diabetes Research Center (FOEDRC) pilot grant to Y.M.U. and by predoctoral fellowships from the American Heart Association, Midwest Affiliate, to M.S.K. and P.R.H. We thank Dr Miyawaki for his gift of the mtPericam plasmid.